NTNU – Trondheim
Norwegian University of
Science and Technology

Treatment of a Waste Water Pharmaceutical by Fenton Oxidation

Paracetamol contaminated Waste Water
treated by the Heterogeneous Dark- and
Photo-Fenton Oxidation

Øyvind Jacob Kjos-Hanssen

Chemical Engineering
Submission date: August 2012
Supervisor: Hallvard Fjøsne Svendsen, IKP
Co-supervisor: Henri Delmas, ENSIACET, Toulouse, Frankrike

Norwegian University of Science and Technology
Department of Chemical Engineering

Abstract

A study within the field of water treatment has been performed, using advanced oxidation processes, namely the heterogeneous dark- and photo-Fenton processes. The applied catalysts were two iron doped zeolites, ZSM-5 (Fe/MFI) and Beta (Fe/BEA).

The treatment of water polluted by paracetamol was studied using a combination of methods of analysis. The degradation of the paracetamol molecule was analyzed by HPLC, while the concentration of aqueous organic pollution was evaluated with total organic carbon (TOC). The oxidant consumption and the magnitude and the activity of leached iron were also investigated.

The kinetics of the experiments varied with the investigated parameters and clear trends were not found, however the three major events were proposed to occur; the oxidation of the aqueous and adsorbed organic molecules, the continuously changing equilibrium between aqueous and adsorbed phase, and the formation of iron-organic-intermediate complexes. The major difference compared to former studies on paracetamol was that the adsorption on the zeolites had a large impact on the kinetics of the processes.

A complete degradation of the paracetamol molecule was obtained in every experiment within 5 to 180 minutes, while the degree of mineralization reached 20-70% in five hours. When going from dark- to photo-Fenton an increase in TOC conversion was observed for both zeolites. The magnitudes were between 15-40% for the Fe/MFI and 14-19% for the Fe/BEA. On the other hand, the increase of oxidant (H_2O_2) concentration affected the TOC concentration of the zeolites differently. The TOC conversion increased between 20-30% for the Fe/MFI while it decreased (between 1-5%) for the Fe/BEA. The activity of the leached iron was of a larger magnitude for the Fe/BEA zeolite than for the Fe/MFI.

The highest degree of mineralization, after five hours of oxidation, based on *the liquid phase* was found to be 68% for the photo-Fenton reactor setup using the Fe/MFI as catalyst at 30°C and an oxidant amount of two times the stoechiometry for full mineralization ($27.7 mmol L^{-1}$). When including the remaining adsorbed organic pollutant the highest degree of mineralization was 60%. This was obtained with the photo-Fenton using Fe/MFI as catalyst at 30°C and ten times the stoechiometry of oxidant ($138.5 mmol L^{-1}$).

It seems that the total biodegradability and toxicity of the reaction mixture after the oxidation was found to be environmentally better than the initial values. Further studies will have to be done to prove this.

Sammendrag

Et vannrensingsstudie ved bruk av avanserte oksidasjons prosesser, deriblandt heterogen mørk- og foto-Fenton prosessene, har blitt gjennomført. De anvendte katalysatorene var to ulike zeolitter dopet med jern, ZSM-5 (Fe/MFI) og Beta (Fe/BEA)

Behandlingen av vann forurenset med paracetamol ble overvåket ved bruk av ulike analysemetoder. Nedbrytingen av paracetamol molekylet ble undersøkt med HPLC og den nedbrytingen av alt organiske materiale ble funnet ved analyse av det totale organiske karbon innholdet (eng.: TOC). Forbruket av oksidasjonmiddel og graden av oppløst katalysator ble også undersøkt.

Det ble ikke funnet noen klare trender ved kinetikken til renseprosessen, men tre hovedhendelser ble identifisert; oksidasjon av vanndige og adsorberte organiske molekyler, likevektsinstillingen mellom vanndig og adsorbert fase, dannelsen av jern-karboksyl-komplekser. Forskjellen fra tidligere renseprosesser er at zeolittene har en enorm overflate som adsorberer store mengder av de organiske molekylene. Dette kompliserer kinetikken.

Fullstendig nedbryting av paracetamol molekylet ble oppnådd i samtlige eksperimenter etter 5-180 minutter, på den andre siden oppnådde den organiske nedbrytningen mellom 20-70% på fem timer. En tydelig forbedring av organisk nedbrytningsgrad ble funnet ved introduksjon av UV-bestråling. Forbedringsgraden var mellom 15-40% for Fe/MFI katalysatoren og 14-19% for Fe/BEA katalysatoren. Ved å tilføre forskjellige mengder oksidasjonmiddel viste de to katalysatorene forskjellig oppførsel. Den største mengden med oksidasjonsmiddel økte nedbrytingsgraden 20-30% for Fe/MFI katalysatoren i forhold til den minste mengden av oksidasjonsmiddel, mens for Fe/BEA katalysatoren sank den organiske nedbrytningsgraden 1-5% ved den største mengden.

Den høyeste oppnådde nedbrytningsgraden, etter fem timer, basert på *væskefasen* ble funnet å være 68%, for foto-Fenton prosessen med Fe/MFI som katalysator, temperatur 30°C og den lave konsentratsjonen av oksidasjonsmiddel ($27.7 mmol L^{-1}$). Ved å analysere katalysatoren for å finne det gjenværende organiske materialet, ble nedbrytningsgraden funnet til å være 60%. Dette ble oppnådd for foto-Fenton prosessen med Fe/MFI som katalysator, temperatur 30°C og den største konsentrasjonen av oksidasjonmiddel ($138.5 mmol L^{-1}$).

Det kunne tyde på at den totale biologiske nedbrytningsgraden og giftigheten på det forurensede vannet etter prosessen ble funnet til å være mer gunstig enn før. Ytterligere studier bør gjennomføres for å bekrefte dette.

Declaration

I hereby declare that the work presented in this thesis has been conducted independently and in accordance with the rules and regulation for the integrated Master's degree in Industrial chemistry and biotechnology at the Norwegian University of Science and Technology (NTNU). The work has been conducted from March to July 2012.

7th August 2012

Øyvind Jacob Kjos-Hanssen

Acknowledgements

The work presented in this thesis has been performed at Laboratoire de Genie Chimique (LGC) at Ecole National Supéuriere en Arts Chimiques et Technologiques (ENSIACET), Toulouse, France, from March to July 2012. The student was doing an exchange year from the Norwegian University of Science and Technology (NTNU), Trondheim, Norway.

I want to thank Filipa VELICHKOVA for the great introduction I was given to the assignnment, and for continuously motivating and helping me. Pray all the best for her future work on the topic. A large thank you goes to my French supervisor Carine JULCOUR who has given me counseling during experiments and interpretation of my results. I also want to thank my professors Henri DELMAS at ENSIACET and Hallvard F. SVENDSEN at NTNU for all their wise counseling during the thesis and for giving me this opportunity to study in France.

"Un grand merci" to Marie-Line DE SOLAN BETHMALE, Marie-Line PERN and Sandrine DESCLAUX for their technical help regarding the analyses. David RIBOUL deserves proper thanks for taking care of the analyses regarding the intermediates. "Je veux aussi donner un grand merci" to Jean-Louis LABAT and Jean-Louis NADALIN for their technical assistance with the experimental setup and to Alan PHILIP for his always helping and never ending good mood.

I want to thank my good friend Hannes for our daily breaks that moved my mind over to other topics. And last but not least I want to thank my dear Kathrine for the wonderful time we have had in France and how she has continuously motivated me during this thesis

---

"Education is what remains after one has forgotten what one has learned in school."

Albert Einstein.

Table of contents

Abbreviations

WWTP	Waste water treatment plant
PNEC	Predicted non-effect concentration
AOP	Advanced oxidation processes
UV	Ultra violet
IUPAC	International union of pure and applied chemistry
TOC	Total organic carbon (apparatus or concentration)
LC_{50}	Lethal concentration (kills 50% of tested animals)
MFI/ZSM-5	Zeolite Socony Mobile
H-BEA/Beta	Beta zeolite
RPM	Rounds per minute
HPLC	High performance liquid chromatography
NA	Non-applicable
GC	Gas chromatography
IC	Inorganic carbon
TC	Total carbon
LGC	Laboratoire de genie chimique
COD	Chemical oxygen demand
HPLC-MS	HPLC (above) coupled with mass spectroscopy

Symbols

Symbol	Explanation	Units
$\mathbf{k_i}$	Reaction rate of reaction i	mol/s, 1/s
X	Zeolite support	-
hν	UV-irradiation	J/s^2
χ_{TOC}	TOC conversion factor/degree of mineralization	-
$\mathbf{C_{TOC,i}}$	TOC-value at time t=i	mg carbon/L
$\mathbf{C_{n,I}}$ **or** $\mathbf{C_i}$	Molar concentration of component i	mol/L
$\mathbf{C_{m,i}}$	Mass concentration of component i	mg/L
$\mathbf{M_i}$	Molar weight of component i	mg/mmol
$\mathbf{V_i}$	Volume of component i	mL
$\mathbf{X_i}$	Mass fraction	-
$\boldsymbol{\rho_i}$	Density of component i	g/L
Ksp	Solubility constant	L^2/mol^2
$\mathbf{K_i}$	Constant for i	-
$\mathbf{A_i}$	Area of i	-
$\mathbf{m_i}$	Mass of component i	g
$\boldsymbol{\sigma_i}$	Standard deviation of i	various
φ	Function for statistical errors	various
$\boldsymbol{\chi_i}$	parameter in the main equation	various

List of Figures

List of tables

1 Introduction

Waste water is treated in several different ways, depending on what it contains. However, the resulting liquid may still contain toxic chemicals, for instance pharmaceuticals. If these pollutants are not removed, they enter the environment and might end up in ecological systems or drinking waters. Although a majority of pharmaceuticals are biodegradable[1], which means that they degrade before leaving the body, or that they will degrade quickly in the environment, they might still persist since they are continuously being discharged from waste water treatment plants (WWTP). The effects this will have on humans, animals and plants have not yet been fully investigated, but preliminary studies show negative effects on affected fish and bacteria[1,2].

Anti-phlogistons are consumed in large numbers, and since many of them also are available without a prescription, like paracetamol, it is plausible that they can be found in the aquatic environment[3]. It has been reported that paracetamol is the most frequently detected at superior concentrations of all pharmaceuticals in French rivers[4]. Concentrations found in the Tyne river in northern England have been between 6,9-69 µg/L[5] and in the outlet of German sewage treatment plants concentrations of 6,0 µg/L have also been found[3]. These values are higher than the predicted non-effect (PNEC) for invertebrates[6], which leads to the conclusion that new treatment methods are needed to minimize the flow to the environment.

Current removal methods of pharmaceuticals are either physical-chemical (settling, flotation) or biological (biodegradation). The studies performed in Germany[3] and in the UK[5], concluded that the current methods for the removal of pharmaceuticals are not sufficient. To improve the removal efficiency advanced oxidation processes (AOP) can be applied. These are methods produce a powerful hydroxyl radical that efficiently breaks down aqueous organic molecules like pharmaceuticals[7].

The work in this thesis will focus on two of these AOPs, namely the heterogeneous Fenton and heterogeneous photo-Fenton reaction using iron doped zeolites as catalysts. An effort will be made trying out different operating conditions to see the effectiveness of the processes.

The thesis starts with the background chapter chronically following the development of the Fenton oxidation. This is meant as a build up of the stepwise buildup of the readers knowledge starting with the theories behind the homogeneous Fenton, before complexing with the heterogeneous Fenton and photo-Fenton processes. The following chapter concerns the materials, the experimental procedures and the methods of analysis, to clarify what

practical work has been done. In the results and discussion chapter assumptions and methods are verified, through calculations and preliminary experiments, before the actual results form the different experiments are presented, compared and discussed. The whole report ends with the conclusion and some proposed further work. The appendices contain detailed calculations, calibration curves and perspectives of the study, and are referred to throughout the thesis.

2 Background

2.1 The Fenton reagent

Although the Fenton reaction today is one of the world's most important oxidation reactions, its discovery was actually a case of serendipity. In 1876 H.J.J. Fenton observed a mixture of tartaric acid, iron (II) salt, hydrogen peroxide and a base, and noted that the reaction resulted in a violet color. The immediate conclusion was that he had found a test for tartaric acid. However, several years later he published a paper [8] regarding the properties this mixture had in oxidation of several organic molecules. In 1934 the topic was again of interest when Fritz Haber and Joseph Weiss discovered that the particular mixture degraded the hydrogen peroxide and produced a hydroxyl radical, $HO^{\bullet}$, and that it was in fact the hydroxyl radical that worked as an oxidant[9]. Today the mixture of an iron(II) salt and hydrogen peroxide is known as the Fenton reagent[10].

Even though the Fenton reagent has been known since the beginning of the last century, its application in wastewater treatment did not occur until the late sixties[11]. After this time it has played an important part within treatment of water polluted with toxic chemicals.

2.2 The homogeneous Fenton reactions

The Fenton reagent plays an important part within the Advanced Oxidation Processes (AOPs). These processes are defined as reactions that involve the generation of hydroxyl radicals in sufficient quantity to affect water purification[12]. The AOPs usually involve a combination of oxidation agents (H_2O_2 or O_3), irradiation (UV or ultrasound) and catalysts (metal ions or oxides)[11].

The hydroxyl radical is the second most powerful oxidant known (second highest oxidation potential known, see Table 2-1). It oxidizes organic molecules non-selectively and produces dehydrogenated or hydroxylated derivatives until their mineralization, i.e. conversion into carbon dioxide, water and inorganic ions.

Table 2-1:Oxidation-reduction potentials of oxidation agents[13]

Redox Reaction	Eo (NHE) volt, 25°C
$F_2 + 2e = 2F^-$	2.87
$OH + H^+ + e = H_2O$	2.33
$O_3 + 2H^+ 2e = O_2 + H_2O$	2.07
$H_2O_2 + 2H^+ + 2e = H_3O_2+$	1.76
$MnO_4- + 4H^+ + 3e = MnO_2 + 2H_2O$	1.68
$HClO_2 + 3H^+ 4e = Cl^- + 2H_2O$	1.57
$MnO_4- + 8H_+ + 5e = Mn^{2+} + 4H_2O$	1.49
$HOCl + H^+ + 2e = Cl^- + H_2O$	1.49
$Cl_2 + 2e = 2Cl^-$	1.36
$HBrO + H^+ + 2e = Br^- + H_2O$	1.33
$O_3 + H_2O + 2e = O_2 + 2OH^-$	1.24
$ClO_2(g) + e = ClO_2-$	1.15
$Br_2 + 2e = 2Br^-$	1.07
$HIO + H^+ + 2e = I^- + H_2O$	0.99
$ClO_2(aq) + e = ClO_2-$	0.95
$ClO^- + 2H_2O + 2e = Cl^- + 2OH^-$	0.90
$H_2O_2 + 2H^+ + 2e = 2H_2O$	0.87
$ClO^{2-} + 2H_2O + 4e = Cl^- + 4OH^-$	0.78
$BrO^- + H_2O + 2e = Br^- + 4OH^-$	0.70
$I_2 + 2e = 2I^-$	0.54
$I_3 + 3e = 3I^-$	0.53
$IO^- + H_2O + 2e = I^- + 2OH^-$	0.49

The *homogeneous* catalytic cycle for the production of hydroxyl radicals with the Fenton reagent follows equation (2.1) and (2.2)[14, 15].

$$Fe^{2+} + H_2O_2 \longrightarrow Fe^{3+} + OH^- + HO^{\bullet} \qquad k_1 = 76 mols^{-1} \tag{2.1}$$

$$Fe^{3+} + H_2O_2 \longrightarrow Fe^{2+} + H^+ + HOO^{\bullet} \qquad k_2 = 0.05 - 0.27 mols^{-1} \tag{2.2}$$

Equation (2.1) produces the powerful hydroxyl radical, $HO^{\bullet}$, by oxidizing the iron catalyst. Further on in equation (2.2) the iron catalyst is regenerated by producing another hydroxyl radical, $HOO^{\bullet}$. This radical has a far lower oxidation potential than the mono-oxygen hydroxyl radical, as can be seen from Table 2-1, where it is not mentioned. The main problem here is that the kinetics of the catalyst-regeneration reaction is several orders of magnitude lower than for the production reaction where it is oxidized. This leads to the conclusion that a high catalyst to oxidant ratio would be important to keep up the production of hydroxyl radicals. However, the overall reaction is not as simple as these two equations, there are several other competing reactions occurring at the same time. For instance the reactions that reduce the amount of active species (scavenging reactions) are given in Eq.(2.3), (2.4), (2.5) and (2.6)[15].

$$H_2O_2 + HO^{\bullet} \rightarrow HO_2^{\bullet} + H_2O \qquad k_3 = 1.2 - 4.5 \times 10^7 mols^{-1} \tag{2.3}$$

$$2HO^{\bullet} \rightarrow H_2O_2 \qquad k_4 = 5.3 \times 10^9 mols^{-1} \tag{2.4}$$

$$H_2O_2 \rightarrow \frac{1}{2}O_2 + H_2O \qquad k_5 = 0.001 s^{-1} \tag{2.5}$$

$$HO^{\bullet} + Fe^{2+} \rightarrow Fe^{3+} + OH^{-} \qquad k_6 = 3\times10^8 mols^{-1} \tag{2.6}$$

These reactions are all either dependant on the concentration of oxidant, the hydroxyl radical and/or the iron catalyst. Seemingly a higher concentration of either the oxidant or the catalyst does not imply an increase of the main reaction rate, given in Eq. (2.1); on the contrary, an increase in catalyst or oxidant concentration could lead to a rapid decrease in the rate of mineralization. A conclusion that can be drawn by looking at the kinetic reaction constants is that when a hydroxyl radical is formed, it reacts further instantly, as the reaction rates for the consumption of radicals are a lot higher than the production of them. The preceding reaction between the organic molecule and the hydroxyl radical is the following[15]:

$$RH + HO^{\bullet} \rightarrow R^{\bullet} + H_2O \qquad k_7 = 10^7 - 10^{10} mols^{-1} \tag{2.7}$$

Comparing this rate with the previous ones, it can be depicted that the radicals formed will not only be consumed in the oxidation reaction, as the rates are similar in magnitude. This further leads to the fact that the stoechiometric amount calculated for the reaction is not always sufficient, as not all of the radicals oxidize the organic molecules, but a lot of them are scavenged. The surplus of hydroxyl radicals therefore reacts in one of the scavenging reactions mentioned above.

Eq. (2.7) produces an organic radical from the pollutant, which reacts primarily in one of the following three paths. It can either be oxidized by a ferrous ion(2+), producing a ferric(3+) ion and a stable oxidized organic molecule or dimerize with another organic radical, to produce a larger molecule than initially or be reduced by a ferric ion, producing a ferrous ion and the original organic molecule[15].

The reaction rate of Eq.(2.7) has a broad range of values. The values of the reactions are at the room temperature, where the Fenton reaction usually performs very well, but by augmenting the temperature there is usually a drop in performance. This has been tied to the activation energy of Eq.(2.5), the decomposition of the oxidant (H_2O_2) into molecular oxygen and water. It has an increasing rate of reaction with increasing temperatures, decaying the mineralization efficiency above 50°C[16]. The same reaction be catalyzed by cations (see section 3.5), for instance by the ferric iron, implying once more that the catalyst concentration should not be excessive.

Among the intermediates are the mono- or poly-carboxylates, which may form complexes with the ferric iron (see Figure 3-2). This deactivates the ion and the overall oxidation rate will be reduced. One of the most studied complexes is the complex formed between ferric ion

and the oxalic acid (ultimate product explained in section 3.1.2). This is one explanation for the decreasing mineralization rate occurring after some time[17].

The factors that the Fenton processes are mainly influenced by are; the concentration and nature of the pollutant, the initial pH and as mentioned earlier the concentration of oxidant and iron ions[16]. The nature of the iron ions is also important as it is only the ferrous ion that catalyses the production of the hydroxyl radical.

The complexity of the reaction system infers that the exact reaction rates of each reaction would be difficult to predict, it is therefore very difficult to know the exact extent of each reaction. Instead, an optimization study can be done, where several parameters can be investigated to obtain the maximum mineralization and other desired maxima.

The main advantages by using the Fenton reagent are[11]:

1. There are no halogenated organic products formed during the oxidation processes as with other oxidants, see Table 2-1.
2. Both iron and H_2O_2 are cheap and non-toxic, in addition H_2O_2 is considered as a green oxidant as its byproduct is H_2O[18].

Although these are good arguments for the homogeneous process, there are some evident problems regarding it as well. To begin with; there is a relative limited pH range, between 2.5 and 5, that has to be complied with[16]. Furthermore, when applying the process to an industrial application there is usually a high Fe^{2+}/H_2O_2 – ratio, to have a high production of hydroxyl radicals. This might however lead to the three following problems. Firstly the ferrous ion can decrease the efficiency of the hydroxyl radicals as it can act as a scavenger, as mentioned earlier. Secondly, a very rapid production of organic radicals may cause depletion of dissolved oxygen and further on reduce the degree of mineralization. Thirdly, a large quantity of iron will result in a big amount of sludge, where the iron has to be separated in order to reduce the environmental pollution and to recycle the catalyst[19]. This is a tedious job and favors the use of a catalyst that is easily separated from the reaction mixture.

2.3 The heterogeneous Fenton reactions

The third problem described above may be solved by using a solid catalyst, which is far easier to separate than the aqueous catalyst, as it can be removed by physical means. The ease of separation resolves both the dumping of iron sludge and the recycling of the catalyst, which are both major drawbacks of the homogeneous process. Some studies have earlier been

performed on organic molecules using solid iron catalysts, and among these were iron doped zeolites[20, 21].

The mechanism of the decomposition of H_2O_2 is not as well established for the heterogeneous process as for the homogeneous process. Where some authors suggest an initial adsorption step of H_2O_2 on Fe(III) sites[22], others suggest the adsorption of organics instead[23]. Regardless of this dispute, the following catalytic reaction cycle has been proposed, where X represents the supporting material.

$$X - Fe^{3+} + H_2O_2 \rightarrow X - Fe^{2+} + HO_2^{\bullet} + H^+ \quad (2.8)$$

$$X - Fe^{2+} + H_2O_2 \rightarrow X - Fe^{3+} + HO^{\bullet} + OH^- \quad (2.9)$$

These proposed reactions are the exact same as for the homogeneous cycle save the supporting material(X). As the confusion prevails about the mechanism of the production of the radical, there are similarly unanswered questions regarding the oxidation reactions, these will be discussed in section 4.3. Also the quantity and contribution of leached iron catalyst is important to study when working with heterogeneous Fenton, as a high degree of leaching will lead to a high loss of catalyst. In addition, if the leached iron ions are responsible for the large part of the mineralization there is little need of the heterogeneous phase.

A study done in 2000 by Centi et al regarding the homogeneous and heterogeneous processes of the Fe^{3+}-species showed that the latter has lower pH sensitivity and that it has a higher rate of degradation than the former. Nevertheless it also promotes a higher consumption of the hydrogen peroxide per mol mineralized, which is negative regarding the economical feasibility of the process[14].

2.4 The photo-Fenton reactions

In the sections 2.2 and 2.3, both the homogeneous and the heterogeneous Fenton processes were described. This section will look at the UV-irradiation effect on the Fenton reactor, and it will briefly describe the additional level of complexity this implies. For the homogeneous photo-Fenton process (wave length <~360nm), there are three major reactions occurring[24].

$$H_2O_2 \xrightarrow{h\nu} 2OH^{\bullet} \quad (2.10)$$

$$Fe^{3+}\left(OH^-\right) \xrightarrow{h\nu} Fe^{2+} + OH^{\bullet} \quad (2.11)$$

$$Fe^{3+}\left(L^{-}\right)\xrightarrow{h\nu}Fe^{2+}+L^{\bullet}\quad\left(L=organic\,ligand\right)\tag{2.12}$$

According to these three equations, it seems clear that UV-irradiation would improve the conversion of the organic pollutants with respect to the "dark" Fenton reactions. Eq. (2.10) is a reaction like none of the other Fenton reactions, giving a pure gain of two hydroxyl radicals per hydrogen peroxide molecule without deactivating the iron catalyst. Furthermore Eq. (2.11) and (2.12) regenerate the ferric ions, while producing a hydroxyl- and an organic radical respectively. The two latter reactions might serve the "dark" Fenton reaction very well, as they break the complexes inhibiting the ferric ion[17] while they also reduce it to produce the ferrous catalyst.

As earlier mentioned the mechanism of the heterogeneous Fenton reaction is not clear. The even more complex heterogeneous *photo*-Fenton reaction has been even less studied. However one phenomenon that might lower the effect of the heterogeneous process, comparing it to the homogeneous process, could be that the solid zeolites will absorb a large quantity of photons since they are not transparent.

To verify the effectiveness of the heterogeneous catalyst in the photo-Fenton experiments, photolysis alone can be performed. In this AOP the hydroxyl radicals are formed from the absorption of a photon in the hydrogen peroxide molecule; however a problem is that the molar absorption rate of hydrogen peroxide feeble (at a wavelength of 253.7nm the molar absorption rate is ~20$M^{-1}cm^{-1}$). A solution that has proven to perform well is operating with high alkaline conditions; this increases the concentration of HO_2^- ions which have a higher absorption rate than the hydrogen peroxide molecules (240$M^{-1}cm^{-1}$)[12].

3 Materials and method

The experiments done in this thesis were carried out with two different iron/zeolite catalysts; Fe/MFI and Fe/BEA. Every experiment had the same initial concentration of paracetamol ($100mgL^{-1}$) and zeolites ($2gL^{-1}$), while the variable parameters were; temperature (30, 45 and 60°C), amount of oxidant (2 or 10 times the necessary stoechiometry for complete mineralization) and with/without the presence of UV-irradiation (medium pressure Hg-lamp - 450W). To discriminate between homogeneous and heterogeneous activity in the reactor, complimentary experiments were run using the filtrated solution from a finished experiment, adding only paracetamol and oxidant.

3.1 Raw materials

3.1.1 Analytical chemicals

The raw materials used are presented in Table 3-1, with information from where they were obtained and their purity.

Table 3-1: Raw materials, including producer and purity

Context	Material	Producer	Purity
Reactants and catalyst	Paracetamol (Acetaminophen)	Sigma-Aldrich	Solid, purity min. 99.0%
	Hydrogen peroxide (H_2O_2)	Fluka Analytical	30wt%
	Fe-MFI -27 (Fe-doped ZSM-5 zeolite)	Süd Chemie	3.57 % Fe on zeolite
	Fe-BEA -25 (Fe-doped Beta zeolite)	Süd Chemie	3.08 % Fe on zeolite
Buffer and inhibitor	Potassium Iodide (KI)	Sigma-Aldrich	Solid, purity min. 99.5%
	Sodium sulfite (Na_2SO_3)	Sigma-Aldrich	Solid, purity min. 98.0%
	Potassium phosphate (KH_2PO_4)	Sigma-Aldrich	Solid, purity min.99.5%
	Sodium phosphate (Na_2HPO_4)	Sigma-Aldrich	Solid, purity min. 99.5%
HPLC	Ortho-phosphoric acid (H_3PO_4)	Fluka Analytical	Conc. ≥85%
	Acetonitrile (CH_3CN)	Scharlau	HPLC grade ≥99.98%
	Methanol (CH_3OH)	Scharlau	HPLC grade ≥99.99%
TOC	Hydrochloric acid (HCl)	Panreac	Conc. 37%
H_2O_2 titration	Potassium permanganate ($KMnO_4$)	Merck	Titrisol $0.02molL^{-1}$
	Potassium oxalate ($K_2C_2O_4$)	Sigma-Aldrich	Solid, purity min. 98.5%
	Sulphuric acid (H_2SO_4)	Sigma-Aldrich	Conc. 95-97%

3.1.2 The pollutant

Paracetamol (see Figure 3-1) also called acetaminophen or by its IUPAC name *N-(hydroxyphenyl)-ethanamide*, is a non prescriptive drug, with pain relieving and fever reducing properties. One of the reasons this pharmaceutical is of interest within waste water treatment, is that it is used in large amounts worldwide. A study by Henschel et al assumed that an annual 292 to 585 tons reaches German sewage treatment plants alone[25].

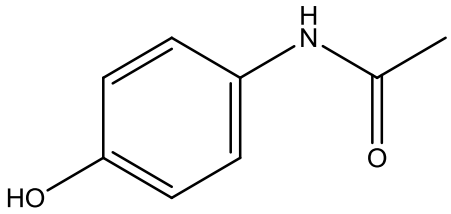

Paracetamol

Figure 3-1: The paracetamol molecule

Paracetamol has been found in substantial concentrations in rivers, downstream of sewage treatment plants, in Germany and the UK[3, 5]. The concentrations ranged from 6.9 to 69 μgL^{-1}, which, according to a Norwegian study[6], includes the maximum predicted no-effect concentration (PNEC) for invertebrates at $9.2\mu gL^{-1}$. The same study also reported that the degree of biodegradation of the paracetamol molecule has been found to be between 57-99% in 28 days. Even though it is readily degradable the continuous discharge of it and the time of degradation mean that it may persist in the environment.

The conventional way of reducing the pollution of chemicals or pesticides today is to prohibit or restrict their uses; however this is neither possible nor desirable as the human benefit often has a higher priority. Instead, to minimize the amount of discharged pharmaceuticals into the environment, special treatment of hospital wastes and separate disposal of pharmaceuticals have been proposed[25].

Studies found in the literature regarding the degradation of paracetamol with AOPs are listed in Table 3-2. The degree of mineralization is also listed to see the effectiveness

Table 3-2: Previous studies on the degradation of Paracetamol using different AOPs

Process	Parameters	Mineralization (TOC) [%]
Continuous homogeneous photo-Fenton[7]	$50mLh^{-1}$ H_2O_2, $C_{Fe(II)}=2mgL^{-1}$, pH=2.5, T=40°C, t=120min	71.5%
Ozonation[26]	T=40°C, $Q_{ozone}=36Lh^{-1}$	30%
H_2O_2/UV[26]	$C_{H2O2}=5x10^{-3}molL^{-1}$, pH=3, T=27°C, t=120min	40%
Homogeneous solar photo-Electro Fenton[27]	$P=32Wm^{-2}$, $C_{Fe(II)}=0.40mM$, pH=3, I=5A, t=120min, T=35°C	75%
Homogeneous Electro Fenton[28]	$C_{H2O2}=16.3x10^{-3}molL^{-1}$, $C_{Fe(II)}=0.087x10^{-3}molL^{-1}$, pH=3, $I=38Am^{-2}$ $C_{paracet}=5mM$	19%
Homogeneous photo-electro Fenton[28]	$C_{H2O2}=14.8x10^{-3}molL^{-1}$, $C_{Fe(II)}=0.08x10^{-3}molL^{-1}$, pH=3, $I=38Am^{-2}$ $C_{paracet}=5mM$	20%

As can be seen in Table 3-2 the degrees of mineralization are not 100%, implying that there are organic molecules still in the solution. Some studies have been performed investigating these intermediates produced from the degradation of paracetamol, either by ozonation (Andreozzi et al in 2003)[26] or by solar photo-electro Fenton (Alemeida et al in 2011)[27]. It was assumed that the degradation mechanism follows that of the latter process, as it is a Fenton process. In Figure 3-2 the mechanism of the degradation is described. The different components were detected either by mass spectroscopy coupled with reversed phase chromatography or by ion exchange chromatography. The results were qualitatively performed using standardized solutions of the products.

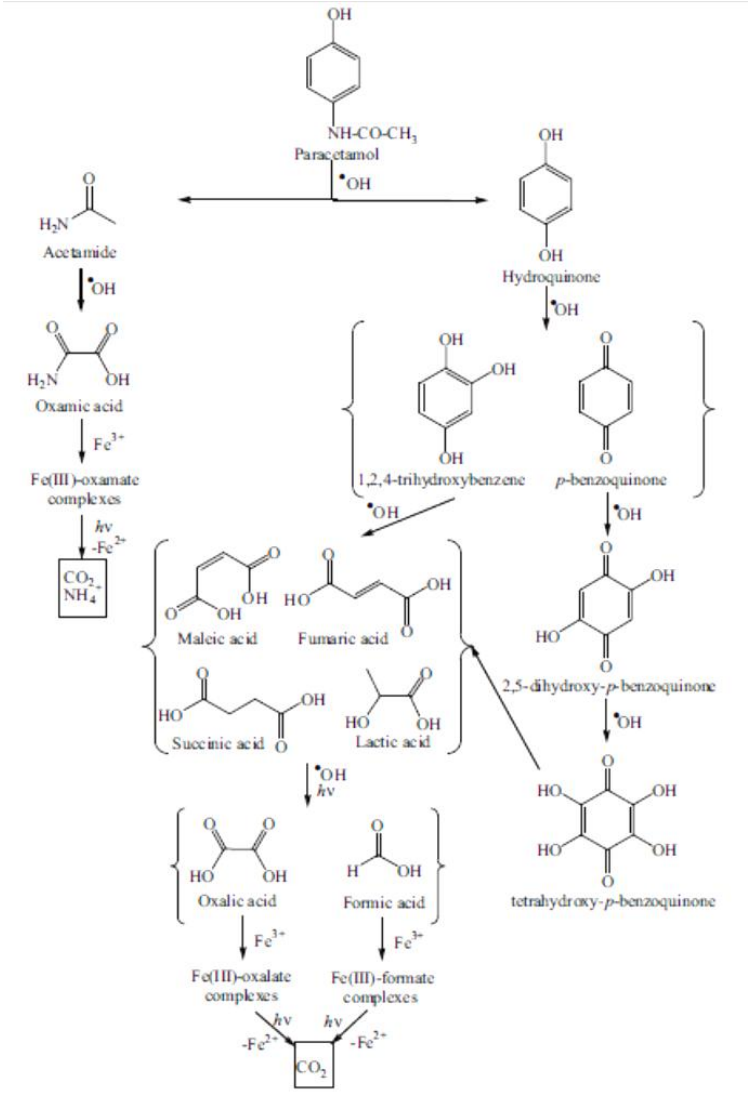

Figure 3-2: Degradation mechanism of the paracetamol molecule using the solar photo-electro Fenton process[27]

The study by Almeida et al found that the aromatics were not measurable after 80 minutes of oxidation, and that the remaining organic molecules were mostly organic acids. The first intermediate organic acids were maleic, fumaric, succinic and lactic acid made from the cleavage of the benzene ring. The ultimate products were; oxalic, formic and oxamic acid that could be directly mineralized to CO_2[27]. Regarding the eco-toxicity of the oxalic acid, it is low as it has a LC_{50}-value of 100ppm (mgL^{-1})[29] which is largely inferior to the concentrations that would appear in the effluents. A study done by Sharma et al found that this acid is readily biodegradable[30]. No information was found on the eco-toxicity or biodegradability of the two other acids. Worth to mention is that in the same study most of the non-aromatic organic acids were found to be degradable, which could be drawn as a temporary solution for the two latter acids. Information on the ecotoxicity on the acetamide was not found, however it is known to be cancerogeneous and its biodegradation products are more toxic than the molecule itself[31].

Another study from Jordá et al in 2011 performed on the necessary degree of mineralization through the photo-Fenton, proposed a degree of mineralization of 18.6% on a solution originally containing 157mgL^{-1} paracetamol. This was proposed to reach the necessary biodegradability of the remaining solution that would be discharged to an ordinary WWTP[32].

3.1.3 The catalyst

When mentioning zeolites and waste water in the same sentence, the conventional thought is with respect to the zeolite adsorption properties. Earlier, the utilization of zeolites has been to extract pollutants from the waste water, without performing an oxidation[33]. But as already mentioned the zeolites may also be used as supports for the iron catalyst in the Fenton reaction. Zeolites have catalytic activities within cracking of long chained petroleum products, but also in fine chemical synthesis where they catalyze rearrangement reactions[34].

Zeolites are crystalline aluminosilicates with an ordered framework structure. The networks are build up from SiO_4 and AlO_4 tetrahedral linked through oxygen atoms[35], and the acidity of the zeolite is dependent on the ratio between the two, resulting in a higher acidity for a higher content of aluminate[36]. Within the zeolite lattice there is a regular array of channels and cavities, giving rise to their large specific surface area and particular adsorption properties.

The *shape selectivity* of adsorption on zeolites is governed by the size and shape of the channels, implying that steric hindrance may admit certain molecules into the lattice, while excluding others[37].

If the zeolite contains different channel systems with different cross sections, *reversed molecular traffic control* can be obtained. This effect occurs when the entering molecules are large and bulky and may only enter through the largest cross-sections, while the smaller product molecules may pass through the circular cross-sections, minimizing or avoiding counter diffusion in the channels[37].

Another possible event is the *product selectivity*, where the product formed is too bulky to leave the cavities. This might happen with the products of the dimerization (explained in section 2.2), as they are larger than the starting point and if it is not further oxidized, it will block the pores, deactivating the catalyst[37].

The main properties that makes the zeolites especially interesting for heterogeneous catalysis are: (1) exchangeable cations, allowing the introduction of cations with various catalytic properties (ferric ions in this thesis), (2) when substituted by H^+ cations they possess a large number of vey acidic sites, (3) their pore diameters are less than 10Å (compared to other porous solids that have pore sizes from 10nm and upwards[38]) (4) and they have pores with one or more discreet sizes[37]. The acidity (2) is the reason why the non-doped zeolites have been used for catalyzing reactions in the petro industry. The fact that the acidic sites are used to catalyze other reactions signifies that the zeolite might not be a neutral catalyst carrier. The following two sections contain the properties of the two zeolites.

3.1.3.1 Structural properties of the MFI zeolite

The MFI-27 zeolite is also called ZSM-5 (Zeolite Socony Mobil – five). It contains two types of channels, both which have ten-member ring openings. One of the channel systems appears sinusoidal (horizontal in Figure 3-3), and has close to circular cross-section (5.4Å x 5.6Å), while the other channel system is straight (vertical in Figure 3-3), perpendicular to the first system and has elliptical openings (5.2Å x 5.8Å)[37]. The silicate-alumina ratio is 27.

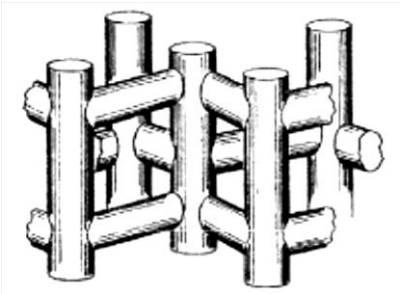

Figure 3-3:Schematic showing the structure of the channels in the MFI zeolite[39]

In an adsorption study by Martucci et al in 2012 the MFI zeolite was tested to see if it had adsorption properties sufficient for pollutant removal from waste water[40]. The conclusion from this was that its adsorptive properties were not acceptable for the three pharmaceuticals investigated as it was below 20 milligram pharmaceutical per gram zeolite of the smallest of the three investigated molecules.

3.1.3.2 Structural properties of the BEA zeolite

The BEA-25 zeolite is also called Beta zeolite. It contains a 12-membered ring pore system with two straight channels, each with a cross-section of 7.6Å x 6.4Å parallel to the [100] (the two vertical channels in Figure 3-4) and the [010] (one horizontal channel in Figure 3-4) direction, and a tortuous channel of 5.5Å x 5.5Å running along the [001] direction (hole in the middle of Figure 3-4). The latter channel is formed by the intersection of the two former channels[41]. The silicate-alumina ratio is 25, so according to Sonnemans et al[36] it should have a higher acidity than the MFI zeolite.

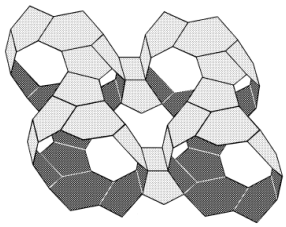

Figure 3-4: Schematic showing the system of channels in the BEA zeolite[41]

3.1.3.3 Specifications

The two zeolites had different specifications, with regards to amount of catalyst and the porosity parameters of the framework. These specifications are given in Table 3-3.

Table 3-3: Iron oxide content, specific surface area and the porous properties of the zeolites

	Iron oxide, Fe_2O_3, content [%]	**S_{BET} N_2 [m^2/g]**	**Vmicro N_2 [cm^3/g]**	**Vmeso N_2 [cm^3/g]**	**Vmacro Hg [cm^3/g]**
Fe/BEA-25	4.4	486	0.14	0.30	0.91
H-BEA-25*	-	554	0.15	0.34	1.08
Fe/MFI-27	5.1	329	0.10	0.05	0.70
MFI-27*	-	377	0.12	0.04	0.98

*Corresponding zeolite without iron

From Table 3-3, the main differences between the two doped zeolites are a slightly higher iron oxide content in the MFI-type than in the BEA-type, a superior specific surface area of the BEA-type (50% larger than the Fe/MFI) and the generally higher void fraction for the BEA-type than for the MFI-type. Regarding the small pore range the BEA has a mesoporous

character while the MFI is mainly micro porous. It is also possible to see a significant decrease of all the parameters when adding the iron oxide. In addition the iron oxide crystals for the Fe/MFI zeolite were probably several orders of magnitude smaller than those of the Fe/BEA zeolite (from CO-chemisorption measurements and X-ray diffractometry).

3.2 Equipment

3.2.1 The Fenton reactor

Two similar glass reactors were used for the heterogeneous Fenton reaction, and were run in parallel. They included; a heating jacket (Fisher Scientific - polystat 71), mechanical stirring, a bottom purge plug, three legged baffles and reactor volumes of 0,5L and 1L. There were two sockets in the lid; one for the mechanical agitation and one for taking samples. Atmospheric pressure was kept throughout the reactions, as the sockets were not sealed, but covered. The mechanical agitation was set to around 350 RPM.

3.2.2 The photo-Fenton reactor

This reactor set consisted of two reactors with heating jackets (Fisher Scientific - polystat 37). The circulation between the reactors was done by a peristaltic pump (Cole-Parmer – Masterflex – 7524-15) with the flow set to 73mL min^{-1}. One of the reactors (0.5 L) contained the Photochemical lamp (ACE Glass Inc. 12128 Photochemical immersion lamp, 450W), a temperature probe, a magnetic agitator and it was kept in a closed safety cabinet. The other reactor, of 1L, was easily accessible for taking samples and had a mechanical agitation set to around 350 RPM. This setup was chosen to have as little irradiation exposure as possible while taking the samples. The lamp had an upper operating temperature of 45°C, hence the upper investigated temperature.

3.2.3 The leachate reactor

This reactor was used to run the experiments on the filtrated reaction solution from an earlier experiment. The design consisted of 400mL Erlenmeyer flasks containing the reaction solutions, a multi-position magnetic stirrer submerged into a heating bath at a controlled temperature (Fisher Scientific – polystat 71).

3.3 Experimental procedures

3.3.1 The Fenton reactor

The paracetamol solution (100mgL^{-1}) was prepared in a volumetric flask (0.5 or 1L), and magnetically agitated for 30 minutes. The heating jacket of the reactor was turned on, and

after this the pH was measured and/or adjusted with sulfuric acid. The solution was thereafter poured into the reactor where it was stirred for 10 minutes. Following was the addition of the solid catalyst, and the mixture was stirred for three hours during the adsorption phase. After this the pH was measured again and the oxidant was added. The oxidation ran for five hours. At the end of the reaction the solid catalyst was separated from the reaction solution. The filtrate setup used a glass filter tube, a 0.22µm cellulose nitrate filter paper and a vacuum pump (ILMVAC - 4000282). The solid catalyst was dried overnight at 70°C (Thermo Scientific - HERAEUS), while the liquid was refrigerated at 4°C.

3.3.2 The photo-Fenton reactor

This procedure was similar to the Fenton reactor, save the circulation pump that was started after the solution and catalyst was poured into the reactor and the UV-irradiation that was turned on 10 minutes before the addition of the oxidant

3.3.3 The leachate reactor

The required amount of paracetamol was weighed in an Erlenmeyer flask (to readjust the solutions paracetamol concentration to 100mgL^{-1}, subsequently approximately 350g filtrated solution from an earlier reaction was added. They were set in a heated bath with magnetic agitation for 10-15 minutes to dissolve the paracetamol, before adding the same amount of oxidant as in the heterogeneous experiment.

3.4 Experimental plan

The experiments carried out during this thesis are listed in Table 3-4. Three temperatures were investigated, 30°C and 60°C had given interesting conversions in earlier studies with heterogeneous Fenton at LGC, and 45°C was the maximum temperature of the photochemical lamp.

The leachate experiments were not done for all of the experiments since the priority was to carry out more experiments. The Fe/BEA did not have the same amount of experiments as the Fe/MFI at 45° C, as proved by the high concentration and the high activity of the leached iron (high conversion of paracetamol and TOC in the leachates).

The photolysis experiments were performed to evaluate the role of iron catalyst in oxidation.

Table 3-4: Experimental plan

Reactor	Temp [°C]	Iron source	Stoechiometric amount H_2O_2 [-]	Leachates
Dark Fenton pH =2.8	60	Fe/MFI	2x	yes
Dark Fenton pH = 2.8	60	Fe/BEA	2x	yes
Dark Fenton	60	Fe/MFI	2x	yes
Dark Fenton	60	Fe/BEA	2x	yes
Dark Fenton	60	Fe/MFI	10x	yes
Dark Fenton	60	Fe/BEA	10x	yes
Dark Fenton	30	Fe/MFI	2x	yes
Dark Fenton*	30	Fe/MFI	2x	no
Dark Fenton	30	Fe/BEA	2x	yes
Dark Fenton	30	Fe/MFI	10x	yes
Dark Fenton*	30	Fe/MFI	10x	no
Dark Fenton	30	Fe/BEA	10x	yes
Photo Fenton	30	Fe/MFI	2x	yes
Photo Fenton	30	Fe/BEA	2x	yes
Photo Fenton	30	Fe/MFI	10x	yes
Photo Fenton	30	Fe/BEA	10x	yes
Dark Fenton	45	Fe/MFI	2x	yes
Dark Fenton	45	Fe/MFI	10x	yes
Dark Fenton	45	Fe/BEA	10x	yes
Photo Fenton	45	Fe/MFI	2x	yes
Photo Fenton	45	Fe/MFI	10x	yes
Oxidation MFI (no iron)	60	NA	2x	NA
Oxidation HBEA (no iron)	60	NA	2x	NA
Photolysis MFI (no iron)	30	NA	2x	NA
Photolysis	30	NA	2x	NA
Photolysis	30	NA	10x	NA
Photolysis	45	NA	2x	NA
Photolysis	45	NA	10x	NA

* The experiment was performed two times because of non-conclusive errors in the analysis.

3.5 Reaction quenching and sampling

The chosen quenching method has been used earlier for similar reactions[42]. To monitor the kinetics of the reactions, two methods of analysis have been used; high performance liquid chromatography (HPLC) and total organic carbon (TOC). To use these methods it was necessary to remove the active species in each sample as they were extracted from the reactor. The oxidant, H_2O_2, had to be reduced, and the dissolved catalyst, Fe^{3+} precipitated and filtered. The two agents used for this purpose are presented in Table 3-5. The inhibitor was used for the TOC samples, while the buffer was used for the HPLC. The reason for excluding

the sodium sulfide and the potassium iodide in the HPLC sample was that they appear as large peaks on the chromatogram. That would disturb the potential of studying the intermediate peaks.

Table 3-5: Scavenging chemicals used for the reaction quenching (buffer and inhibitor)

Solution name	Chemical	Concentration [mol/L]
Buffer	KH_2PO_4	0.05
	Na_2HPO_4	0.05
Inhibitor	KI	0.1
	Na_2SO_3	0.1
	KH_2PO_4	0.05
	Na_2HPO_4	0.05

The iodide ion is responsible for the reduction of hydrogen peroxide, Eq.(3.1), and for the acceleration of H_2O_2 degradation, given in Eq.(3.2):

$$2H^+ + 2I^- + H_2O_2 \rightarrow I_2 + H_2O \tag{3.1}$$

$$H_2O_2 \xrightarrow{KI} H_2O + 1/2\,O_2 \tag{3.2}$$

In addition the iodide ion is also able to reduce peroxide radicals and hydro peroxides into water and alcohol:

$$R-O-O-H + 2H^+ + 2I^- \rightarrow I_2 + H_2O + R-OH \tag{3.3}$$

The sodium sulfite is primarily added to regenerate the formed elemental iodine, Eq. (3.4), while it is also capable in reducing the hydrogen peroxide, Eq.(3.5):

$$Na_2SO_3 + I_2 + H_2O \rightarrow Na_2SO_4 + 2HI \tag{3.4}$$

$$Na_2SO_3 + H_2O_2 \rightarrow Na_2SO_4 + H_2O \tag{3.5}$$

The assumption that the oxidant is poorly active in the absence of iron ions was therefore made, and checked in a preliminary study: after 72 hours of contact with sole H_2O_2, paracetamol conversion was <1%. Nevertheless the HPLC analyses were performed in the same day as the experiments .The two different phosphates precipitate the dissolved Fe^{3+}, as $FePO_4$ has an extremely low solubility in water ($K \approx 5 \cdot 10^{10}$ $L^2 mol^{-2}$), and can therefore be removed by filtration (filter: Millipore 0.22 µm).

Sampling procedure

HPLC samples were taken at 0, 30, 60, 120, 180 minutes of the adsorption, and at 5, 10, 60, 180 and 300 minutes after starting the oxidation. TOC samples were taken at 0 and 180 minutes of the adsorption and at 5, 10, 60, 180 and 300 minutes after starting the oxidation.

A sample of 8 ml was extracted from the reactor with a syringe. The sample solution was filtered with a 0.22 µm nylon filter and thereafter it was distributed into two different syringes. One syringe containing 0.6 ml "buffer" solution was filled to a total of 2mL for the HPLC analysis, and the other syringe containing 2mL "inhibitor" solution was filled to the total of 8mL for the TOC analysis. The samples were thereafter filtered with a 0.22 µm nylon filter to remove the precipitated iron, before the samples were inserted into their respective containers for analysis. In addition the TOC sample was diluted by a factor of 5 with ultra pure water (ELGA – PURELAB – Option-Q).

The measurements done for the preparation of the samples (amount of buffer/inhibitor, reactor sample and dilution) were mass based (Mettler Toledo – New Classic MS, ±0.1mg).

3.6 Methods of analysis

As earlier mentioned the main goal of the Fenton reaction is to degrade the paracetamol content in the water into carbon dioxide and water. There are several different methods of measuring the extent of this reaction, either by looking at the consumption of the reactants or by measuring the amount of accumulated products. As no single method of analysis may give a clear picture of the extent of the reaction, the results from several methods should be compared to see if they give the same conclusions.

To monitor the development of the reaction, samples from the reactor are analyzed. The two main points of interest are; the degradation of paracetamol and the degradation of the total organic compounds. Thanks to liquid chromatography, it is simple to measure the exact concentration of a specific component in a solution. Therefore the HPLC is used to survey the degradation of paracetamol. However, keeping track of all the degradation products in the reactor is cumbersome with the HPLC, since one would have to identify and develop a specific method for every single intermediate. A less time consuming method of analysis uses the elemental analysis of carbon, obtaining the concentration of total organic carbon (TOC) in the reactor. This will give a better picture of the total degradation than the HPLC. In addition, the combination of TOC and HPLC may give information about paracetamol degradation during the adsorption phase, before the addition of oxidant.

To verify these two main methods of analysis and to enlighten other aspects of the process, other methods were also used; the consumption of the oxidant (H_2O_2), the amount of leached iron, the carbon content the solid catalyst.

Table 3-6: Apparatus used for analysis

Method	Module	Name
HPLC (Spectra system)	Solvent delivery	AS1000XR
	Injector	P1000XR
	Detector	UV2000
HPLC (Varian ProStar)	Solvent delivery	Model 230
	Injector	Model 410
	Detector	Model 310
COT (SHIMADZU)	Injector	ASI-V
	Analyzer	TOC-V-CSN
pH –meter (Consort)	Multi parameter analyzer	C861

3.6.1 Degradation of paracetamol

Chromatography is one of the most used methods of analysis for the identification and quantification of compounds in a liquid or a gaseous state. The principle is based on the concentration equilibrium of the components of interest between two immiscible phases. The stationary phase is immobilized within a column, and the mobile phase is forced through the first. These phases are carefully chosen so that the components of the sample have differing solubility in each phase. Thereafter the separation is a function of: length of column, choice of mobile phase, temperature and pressure. Altering the mobile phase composition ratio, may change the resulting separation. The choice of mobile phase can be done in two ways, either; a constant ratio throughout the analysis, called *isocratic*, or a constantly changing ratio called an *elution gradient*. The elution gradient gives a more definite separation than the isocratic mode, which is important if there are a lot of similar products in the sample, nonetheless it is also a lot slower than the isocratic mode[43].

Although gas chromatography (GC) often is the choice when dealing with very low concentrations (as in this project), it is constrained by the fact that the sample has to be vaporized before analysis. As the sample contains mainly water, the HPLC is better suited than the GC due to the fact that water has an extremely large vaporizing volume that may cause problems in the GC[44].

As the HPLC was not going to analyze the intermediates but only focus on the paracetamol concentration, a fast analysis method[45] was utilized. An isocratic mode was applied to save time, with a ratio of 90% acidic water (adjusted to pH=2 with phosphoric acid) and 10%

acetonitrile. The column was a ProntoSIL C18, with a length of 25mm and a diameter of 2.5mm. The flow rate of the mobile phase was 1mL min^{-1}, the temperature 30°C, the runtime 10 min and the detected wavelengths were 210 and 254nm. The calibration curve is shown in Appendix A. It was checked by performing analyses at different wavelengths that no co-elution occurred for the paracetamol peak.

3.6.2 Total degradation of organic pollutants

Due to the need of accuracy and rapidity of analysis in several fields, where chromatography would be too slow, difficult or expensive, elemental analyzers have been developed. These machines are only quantitative, and give the concentration of one or more elements within one sample, rater than displaying the individual components. The principle behind Total Organic Carbon is first to remove the inorganic carbon from the sample by lowering its solubility, and subsequently to oxidize all the remaining carbon within the sample and measure the amount of CO_2 produced. This gives a result proportional to the total organic carbon in the sample[43].

The three definitions that must be distinguished are:

- Total Organic Carbon, TOC: The covalently bonded (organic) carbon
- Inorganic Carbon, IC: The dissolved (inorganic) carbon species
- Total Carbon, TC: The sum of organic and inorganic carbon

The apparatus used in this work, divided the sample in two and measured the TC and IC separately. The TOC value was thereafter obtained by subtracting the IC value from the TC value. The IC value is found by adding a strong acid (HCl, 0.2 M) to the sample; this lowers the solubility of the aqueous inorganic carbon, so that the entire IC vaporizes. The TC value is found by injecting the sample into a high temperature (680°C) oven containing a platinum catalyst with an excess of pure oxygen. The resulting CO_2 in both cases is measured with an infrared detector.

The method used for the TC had two injections, with a maximum of three, if the standard deviation was too high (>2% - the values of the standard deviations were not explicitly given from the TOC-apparatus, so the standard deviations used in Results and discussion are 2% of the original value). The injection volume was 20µL and a calibration curve from 0 to 18mgL^{-1} was used (see Appendix B). For the IC method the same injection procedure was used, with the same volume and using 2% 0.2M HCl. The calibration curve used was from 0 to 3mgL^{-1}.

The catalyst after the reaction was filtered from the solution, and to investigate the amount of pollutant absorbed on it, samples of the catalyst from some reactions were analyzed by trace

carbon analysis, which is a solid TOC analyzer. It uses the same principle as the liquid TOC, but has the sample in solid phase instead of liquid phase. The analyses were performed at; *CNRS, Service Central d'Analyse, Echangeur de Solaize, Chemin du Canal, 69360 Solaize*.

3.6.3 Consumption of oxidant

The oxidant is the main reactant needed to carry out the experiment. Its consumption is therefore interesting as it gives a picture of how effectively the process uses the oxidant. The comparison of the amount of consumed oxidant to the conversion of the organic pollutants reveals if is being consumed proportional to the stoichiometry or not (the stoechiometric amount of oxidant is calculated in Appendix C, using the initial concentration of paracetamol and the equation for the total oxidation to CO_2, H_2O and HNO_3^-).

The concentration of aqueous H_2O_2 can be found by titrating it with potassium permanganate in the presence of sulfuric acid (the standardization of potassium permanganate is given in Appendix D). This titration follows Eq.(3.6).

$$2MnO_4^- + 5H_2O_2 + 6H^+ \rightarrow Mn^{2+} + 5O_2 + 8H_2O \tag{3.6}$$

The permanganate ion, MnO_4^-, has a strong violet color, while the maganate ion, Mn^{2+}, has no color. Therefore the slightest color change indicates that an equal molar amount of permanganate has been added. The amount of consumed H_2O_2 is calculated from Eq.(3.7).

$$X_{H_2O_2}^{consumed} = \frac{n_{H_2O_2}^0 - n_{H_2O_2}}{n_{H_2O_2}^0} = \frac{n_{H_2O_2}^0 - \frac{2}{5} \cdot C_{MnO_4^-} \cdot V_{MnO_4^-} \cdot \frac{M_{H_2O_2}}{C_{H_2O_2 in 30\% H_2O_2} \cdot \rho_{30\% H_2O_2}}}{n_{H_2O_2}^0} \tag{3.7}$$

3.6.4 Leached iron

During the experiment there is always some solid iron that leaches into the solution that might be capable of catalyzing the reaction. This concentration of leached iron can be measured thanks to the Inductively Coupled Plasma-Optical Emission Spectrometry (ICP-OES). The principle of this method is; the sample is exposed to a very high temperature (6-7000K) leading to plasmafication of the atoms (atom is liberated and excited). When returning to their previous state the atoms emit a photon that has a characteristic wavelength, and its intensity is proportional to the number of atoms in the sample. By detecting the wavelength and the intensity a quantitatively measurement of the element in question can be made.

3.6.5 Choice of pollutant concentration

As mentioned earlier, the concentration of paracetamol found in water treatment plant effluents and in water ways ranged from 6.9-69µgL^{-1}. However, the initial concentration used in this work was 100mgL^{-1}. The reasoning for this choice was that the concentrations in reality were so feeble that the analyses with the HPLC and the TOC could not have given satisfying results. In short; accuracy, low cost and low time consumption was prioritized over reality. However, the findings of this work might still be applicable to pharmaceutical wastewater where the concentrations are a lot more substantial[46], COD values up to 362000mgL^{-1}.

4 Results and discussion

The results and discussion is built up by first introducing the preliminary experiments and the verification of the methods of analysis used. Thereafter the phenomena occurring during the adsorption phase are discussed, looking into if the degradation of paracetamol started before the oxidant was added. Further on trends are studied by varying one parameter at a time, and see how it affected the paracetamol oxidation kinetics. Afterwards the degree of mineralization is investigated. The chapter finishes with a short study of the intermediates produced.

4.1 Methods verification and preliminary experiments

4.1.1 Inhibitor and buffer solution

To estimate the effect of the reaction quenching, stoechiometric calculations were made (see Appendix E) using the scavenger concentrations of the buffer and inhibitor and the stoechiometric coefficients from the quenching reactions Eq.(3.1), (3.3) and (3.4). The values presented in Table 4-1 show the initial amount of scavengers in the sample syringes and the calculated surplus of scavenger according to the two oxidant concentrations.

Table 4-1: Calculated values for the reaction quenching

I^-	0.00020	mol/sample
Na_2SO_3	0.00020	mol/sample
H2O2 - 10x	0.00083	mol/sample
H2O2 - 2x	0.00017	mol/sample
Inhibitor at H2O2 - 10x	-64.0	% Scavenger surplus
Inhibitor at H2O2 - 2x	80.2	% Scavenger surplus

Regarding the reduction of the oxidant in the TOC sample, the calculated results were satisfying when the sample contained two times the stoechiometry of oxidant. For the samples with ten times the stoechiometry of oxidant, the available oxidant scavengers were not represented in sufficient amounts to reduce the oxidant according to the same reactions. However, the iodide ion was also able to catalyze the decomposition of the oxidant, see Eq.(3.2) . As its reaction constant was not known, it was not possible to calculate if the added inhibitor actually would remove the excess oxidant. As the oxidant appeared on the HPLC, the verification if the oxidant was efficiently removed was proven by analyzing a solution of water and oxidant, in the same ratio as from the reactor, with and without the inhibitor (shown in Appendix F).

The values calculated in Appendix E for the precipitation of iron, took into account the concentration of phosphate and the solubility constant. The result showed that the diminution of the concentration of the iron ions was sufficient. The measured maximum concentration of ferric ions was 4mgL^{-1} and according to the calculations the phosphate ions would lower the concentration to 4-5·10^{-5}mgL^{-1}, which means it would be reduced by a factor 10^{5}.

The assumption that of one gram equals one milliliter at room temp was made. It was further theoretically proven in Appendix F by using densities of the inhibitor and buffer solution compared to water. The calculated error by assuming this was found to be less than 0.5%.

The sample volumes had a small impact on the oxidant concentrations of the experiments. But due to the fact that the different experiments were carried out in the same manner the error was neglected (also shortly described in Appendix E).

4.1.2 Control of calibration curves

The calibration curves for the HPLC and the TOC are presented in Appendix A and Appendix B respectively. For the HPLC new calibration curves were made for each analysis, with a set of five known solutions run before and after the reaction samples, and only a minor change was experienced from analysis to analysis. In addition the initial sample was compared to the prepared value.

The TOC had an internal calibration curve which was used throughout the thesis. It was controlled by three known solutions at every analysis, if the analyzed values deviated too much (>5%) from the known values a recalibration was made with the three known solutions.

4.1.3 Degree of mineralization

For most of the experiments only the liquid TOC values were measured, henceforth the liquid based degree of mineralization from each experiment was calculated using Eq. (4.1).

$$X_{TOC} = \left(1 - \frac{C_{TOC,t=480}}{C_{TOC,t=0}}\right) \cdot 100 \qquad (4.1)$$

The TOC value was used, since the paracetamol conversion was completed in each experiment. Although this method was chosen to calculate the conversion factor, it did not give the correct value as there may have been still some pollutants adsorbed on the zeolites after the oxidation phase. The true degree of mineralization would therefore have been lower than the calculated one. To be able to compare the results of the experiments done with each other, it was assumed that the remaining adsorbed pollutants in equilibrium with the amount

of aqueous pollutants for similar temperatures. Hence the experiment with the highest degree of mineralization had the lowest concentration of adsorbed pollutant.

To be able to compare the end values from different temperatures it had to be taken into account that; adsorption capacity decreased with increasing temperatures; also the adsorption on the Fe/MFI and Fe/BEA, where the latter had a superior adsorption capacity during the adsorption of paracetamol. Assuming that the adsorption capacity followed similar trends for the intermediate molecules as for the initial molecule the following points were made:

- The experiments performed at a low temperature had an overestimated degree of mineralization compared to the experiments performed at a higher temperature.
- The experiments with Fe/BEA zeolite an overestimated degree of mineralization compared to the experiments with the Fe/MFI zeolite.

4.1.4 Determination of the duration of the experiment

Before starting the oxidation it was crucial to ensure that the reaction had reached equilibrium, as the aqueous pollutant concentration decreased due to both oxidation and adsorption. To be sure that every oxidation experiment would start at similar values after the adsorption, they were run for 180 minutes before adding the oxidant. At this point the concentration had stabilized and there was little change from there on, see Figure 4-1. The continuing increase/decrease in paracetamol concentration will be further studied in section 4.2.

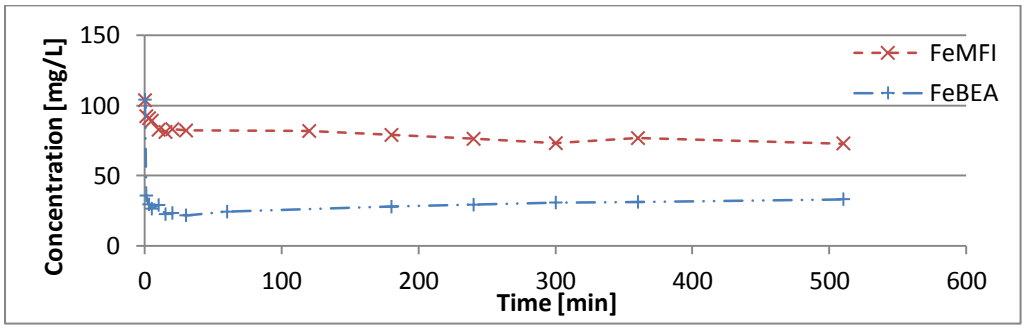

Figure 4-1: Adsorption experiments for the different iron doped zeolites run at ambient temperature

The duration of the oxidation reaction was set to five hours, this way each experiment lasted ten hours including preparation and shut down procedures.

4.1.5 Preliminary experiments

Before embarking on the experimental plan, some preliminary experiments were carried out. These first experiments were done for several purposes; as a validation of the methods of analyses, to clarify if the zeolites would give a conversion worth a more thorough investigation and to investigate the significance the initial pH has on the reaction.

The conditions for these experiments were 60°C, two grams zeolites per liter, two times the stoechiometry of H_2O_2 and each zeolite was investigated at natural- (not adjusted) and adjusted pH; altogether four experiments. The experiments were run in the Fenton reactor.

As the prepared concentrations differed, the values used for the plot, Figure 4-2, were first normalized to an initial concentration of 100mgL^{-1}. These non-similar initial concentrations were later prevented by enforcing a higher accuracy when preparing the solution.

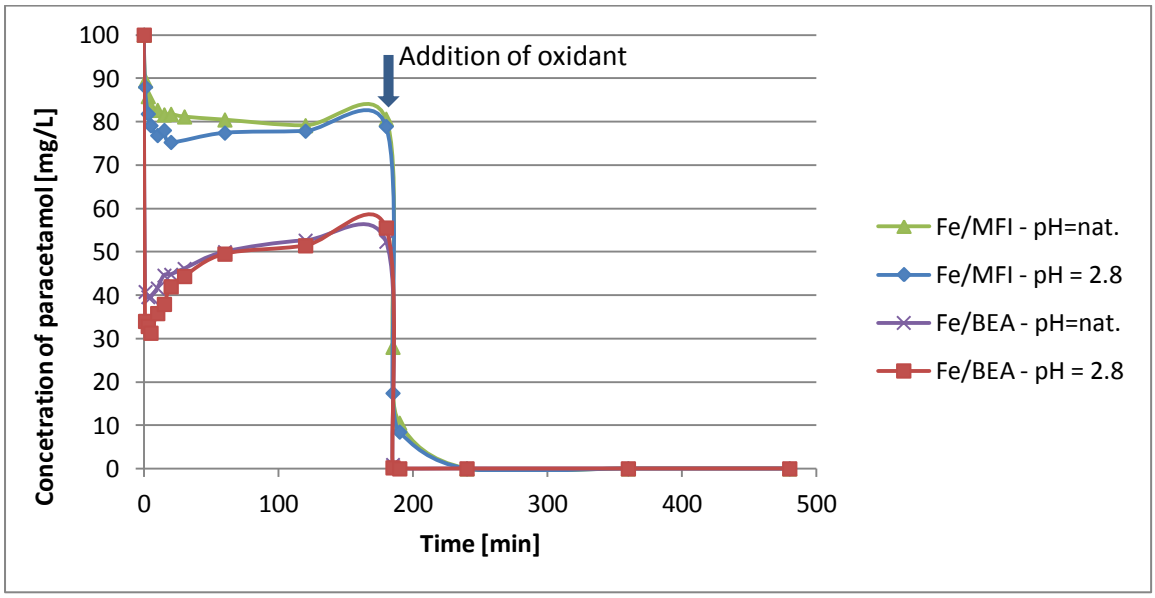

Figure 4-2: HPLC analyses of the adsorption (0-180 min) and oxidation (180-480 min) of Fe/MFI and Fe/BEA at 60°C, pH=2.8 and natural and 2X stoechiometry of H_2O_2

It can be depicted from Figure 4-2 that the paracetamol was degraded quickly in all four cases. For the Fe/BEA catalyst the time of total degradation was less than 10 minutes, while the Fe/MFI catalyst yielded a slower degradation of paracetamol of between 10 to 60 minutes. The rapid degradation indicated that the HPLC analyses were mostly for qualitative purposes during the oxidation.

During the adsorption phase it was possible to see two significantly different behaviors for the two catalysts, as will be discussed later in section 4.2. Very similar trends were repeated for each catalyst, which implies that the adsorption and degradation of the paracetamol molecule did not have a high dependency on the initial pH. This corresponds well with the conclusion of Centi et al from 2000[14] that was a small pH-dependency of the heterogeneous catalyst.

By further looking at the values from the TOC analyses, a clearer picture was made of how the total degradation in the reactor proceeded. The results from the HPLC showed that the paracetamol degrades quickly, but by looking at Figure 4-3, it was obvious that this degradation had resulted in intermediates and that the overall degradation was slower than as it had seemed from the HPLC values.

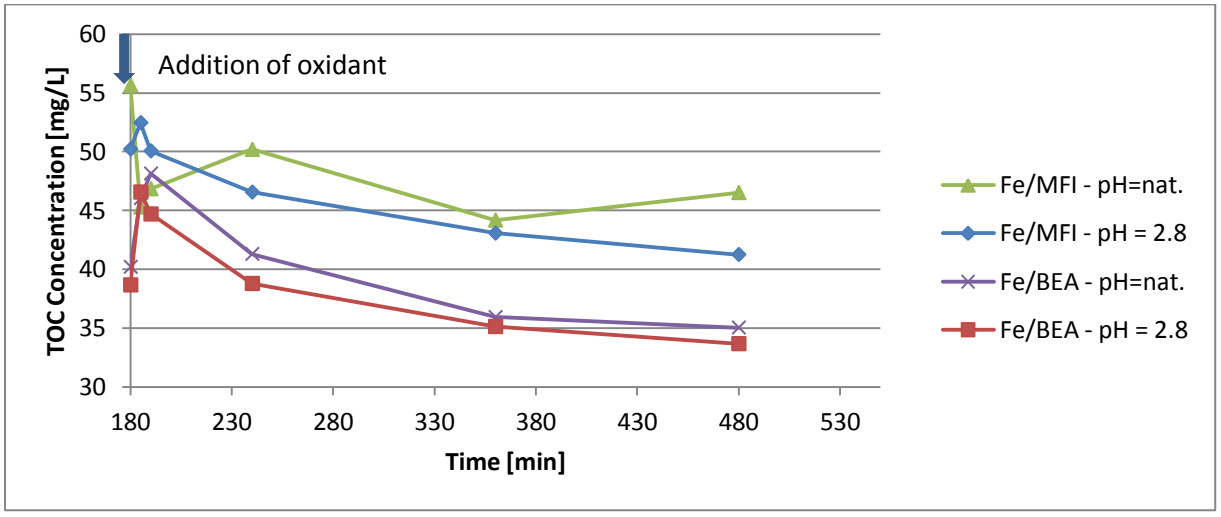

Figure 4-3: TOC values analyses of the oxidation (180-480 min) of Fe/MFI and Fe/BEA at 60°C, pH=2.8 and natural and 2X stoechiometry of H_2O_2

The Fe/BEA had a clear and very similar trend in the two experiments during the oxidation. The curves for the Fe/MFI were however not as similar. One explanation for this could have been drawn from fact that they had different initial TOC concentrations. The trend for the experiment with Fe/MFI at natural pH differed from the three other experiments in that the addition of oxidant resulted in a momentarily descend in TOC value, where the others had an increase of TOC value after the addition. The increase could be explained as a competitive adsorption between the physisorbed paracetamol and the oxidant. However the drop in TOC value might have been a sample preparation error.

To recapitulate; the primary goal of the experiments was to degrade as much as possible of paracetamol and its oxidation intermediates. As discussed earlier, the two zeolites were able to degrade all the paracetamol at the given conditions. However the TOC conversions (based on liquid phase) for the Fe/BEA were superior to the Fe/MFI, see Figure 4-4.

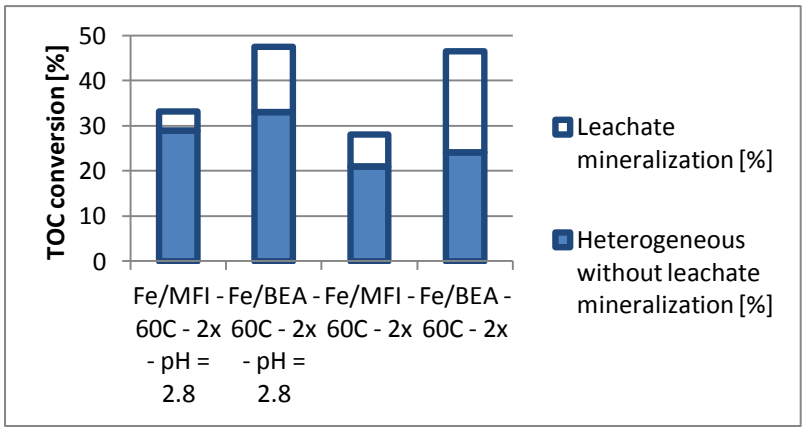

Figure 4-4: Degrees of mineralization of the heterogeneous and leached phase for the preliminary experiments

Each whole bar (combined blue and red) in Figure 4-4 represents the degree of mineralization from the heterogeneous experiments, while the upper not filled part is the contribution from the leached experiment. It can further be depicted that the Fe/BEA had a significantly larger leachate contribution than the Fe/MFI, from this it was assumed that there was a significant amount of iron acting as catalyst in these experiments. This assumption was further reinforced by comparing it to the concentration of dissolved iron from each reactor, where the Fe/BEA had a superior concentration of leached iron in both cases, and a up to 6% of the total iron leached form the Fe/BEA zeolite, see Table 4-2. This finding resulted in increased interest in the Fe/MFI as it would suit better for a continuous process than the Fe/BEA, due to the fact that less catalyst would be lost from catalyst leaching. Also the Fe/BEA would be dependent on the leached iron to achieve the superior degree of mineralization.

Table 4-2: Analyses of oxidant consumption and dissolved iron concentration for the preliminary experiments

Analysis	**Fe/MFI - pH = 2.8**	**Fe/BEA - pH = 2.8**	**Fe/MFI - pH nat.**	**Fe/BEA - pH nat.**
H_2O_2 consumption [%]	95.3	80.6	92.2	49.0
Iron [mg/L] ([% loss of catalyst])	1.57 (2.20)	3.66 (5.94)	1.04 (1.46)	2.01 (3.26)

The higher iron concentration in the experiments with low pH followed basic chemistry. On the other hand the fact that the smaller quantity of leached iron in the reaction with the natural pH gave a higher leachate conversion in both cases was peculiar, as the homogeneous Fenton reaction usually performs best at lower pH values and higher iron concentrations. One explanation found in literature[17] might be a higher formation of iron-carboxylated complexes for the lower pH value, leading to a higher amount of deactivated iron ions. The optimal pH value of the homogeneous Fenton oxidation was proposed by Garcia-Riojas[16] to be somewhere between 2.5 and 5 depending on the process. This would imply that the non-adjusted pH was closer to the optimum. This implication, however, is not obscure as the zeolites have acidic properties giving the non-adjusted solution a pH from 3.5 to 4 (measured in later experiments). In the other experiment the pH was adjusted before the addition of zeolites, leading to an even lower pH value after the addition of zeolites.

4.1.6 Blank experiments

Six other preliminary experiments were carried out, so called blanks. These experiments were run at the same conditions as the ones containing the iron-doped zeolites, but they were run without iron or without the solid phase. These were run to see the effect of the zeolite itself had and the effect of the UV-irradiation with no iron catalyst present.

Table 4-3: Experiments run with natural zeolite (dark and photo Fenton) and experiments runs without solid phase in the photo-Fenton reactor and their conversions

Experiment	Degree of mineralization COT [%]	Degree and time of total paracetamol degradation	Iron content [mg/L]
MFI - 60C - 2x stoech. H_2O_2	Not Analyzed	100% (<210 min)	Not Analyzed
HBEA - 60C - 2x stoech. H_2O_2	Not Analyzed	78.9% (>210 min)	Not Analyzed
Photo-MFI - 30C -2x – pH=5-6	17.9	96.5% (>300 min)	0.15
Photolysis*(noH_2O_2) - pH=5.5	0	35.3% (>300 min)	Not Analyzed
Photolysis*(noH_2O_2) - pH=2.6	0	4.5% (>300 min)	Not Analyzed
Photolysis*– 2xH_2O_2 - pH=2.6	2.2	89.2% (>300 min)	Not Analyzed
Photolysis* – 3xH_2O_2 - pH=2.6	17.0	98.0% (>300 min)	Not Analyzed

*Experiments run by a different person, when the photo-Fenton setup was purchased

As can be seen from Table 4-3 the pure zeolites were able to degrade the paracetamol without the help of the iron catalyst. This means that the zeolite is not a neutral catalyst carrier.

Regarding the photolysis experiments carried out when the setup was new, it is possible to see that the degree of mineralization and degradation of paracetamol were close to none-existant, for the oxidant free experiments, and relatively feeble for the oxidant containing experiments. The superior degradation of paracetamol at the higher temperature follows the theory of Glaze et al[12], about the content of the higher photon absorbing species of the oxidant.

4.1.7 Section summary

During this section, the methods for performing and analyzing the experiments were accepted, under certain conditions. Both zeolites had a high degree of mineralization motivating the pursuit of the further investigations.

The further focus in this thesis was primarily on Fe/MFI experiments at natural pH, as it had a lower concentration of leached iron than the reaction with the adjusted pH. Other advantages by not adjusting the pH are; avoiding the additional cost of acid addition, the reduced corrosion properties of the solution would have on reactor and materials and avoiding the need for neutralizing the outlet afterwards.

The Fe/BEA was also investigated further because of a high degree of mineralization combined with a lower H_2O_2 consumption than the Fe/MFI.

4.2 Adsorption

All the experiments were affected by the adsorption properties of the zeolites. First of all the actual initial concentration of the oxidation reaction was altered during the adsorption phase, depending on the type of zeolite, the temperature and reactor setup. This section will discuss which adsorption phenomena occurred during the adsorption phase and during the oxidation reaction. The results from the two zeolites are discussed separately.

Adsorption is the accumulation of molecules on the surface of a solid or a liquid. There are two typed of adsorptions possible, either; physical adsorption (*physisorption*) and chemical adsorption (*chemisorption*). The former adsorption event is when a molecule attaches to a surface by means of weak molecular interaction (van der Waals forces), which will mostly be the case for the non-ferric sites of the zeolites as they are largely superior to the ferric sites. This adsorption is non-reactive, meaning the physisorbed and the aqueous molecules are identical. As physisorption is an exothermic reaction, the magnitude of it is inversely depending on the temperature. A slow equilibrium might be caused by a rate determining transport process[47].

The latter type of adsorption is the irreversible chemical reaction between an aqueous molecule and a solid adsorption site[47]. The decomposition of hydrogen peroxide and the production of the peroxide radical on the ferric/ferrous sites is an example of chemisorption.

4.2.1 Fe/MFI

The adsorption phase of the Fe/MFI followed a logical trend; most of the adsorption occurred within 10 to 20 minutes and then smoothed out with a slight slope, Figure 4-5. The main type of adsorption occurring was probably physisorption, as the quantity of non-ferric sites was largely superior to the quantity of ferric sites.

The different temperatures resulted in different final concentrations, where the adsorption capacity was disfavored by an increase in temperature, which correlated well with the literature. There was also a difference in the trends between the Fenton and the photo-Fenton reactor. This could be explained by looking at the two reactor setups, as the photo-Fenton reactor consisted of two separate reactors. As earlier written in section 3.2.2, the zeolites were added to one of the reactors and the reaction solution was thereafter circulated between them. This resulted in a delay in the zeolite concentration equilibrium between the two reactors of approximately 20 minutes (simulated in Appendix H), which resulted in a slightly different adsorption curve.

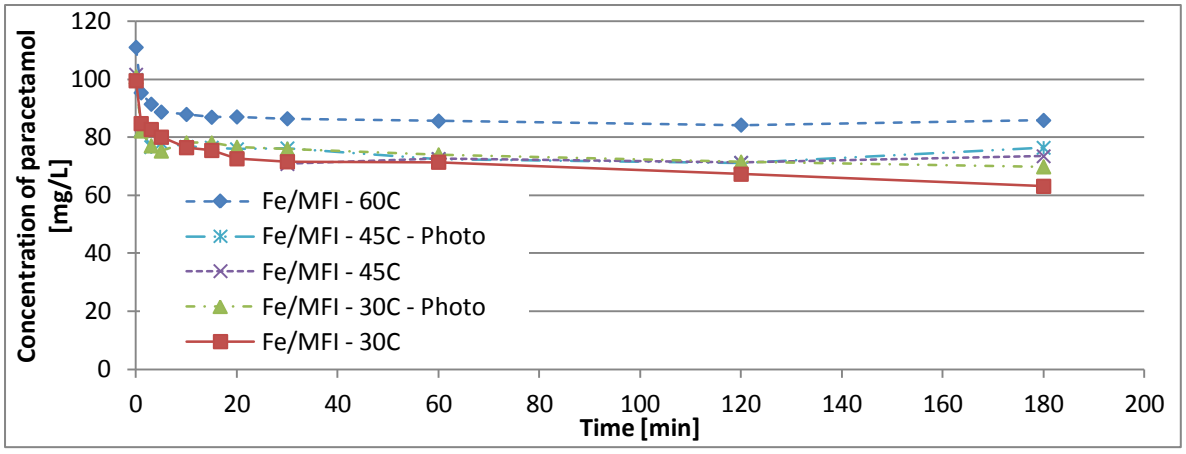

Figure 4-5: HPLC values for the adsorption of paracetamol on the Fe/MFI zeolite at temperatures: 30, 45 and 60°C

Where the Fenton reactor had a continuously decreasing paracetamol concentration from the start, the photo-Fenton reactor had a decrease the first five minutes larger than the Fenton reactor. This could be explained by a zeolite concentration superior to $2gL^{-1}$ in the photo-Fenton reactor that the samples were taken from. After that the concentration of paracetamol increased for about 10-15 minutes, before the concentration in the two reactors followed a similar decreasing trend to the end of the adsorption phase.

The fact that the adsorption curve did not stabilize at a constant concentration, but rather decreased could have induced one of the following; Everett[47] proposed that a slow equilibrium could be caused by a rate determining transport process, the other reason could have been that there were additional phenomena to the adsorption of paracetamol occurring. This could have been a degradation of the paracetamol molecules. This was investigated by comparing the TOC values to the HPLC values, see Table 4-4 (the HPLC values were converted from $mg_{paracetamol}L^{-1}$ to $mg_{carbon}L^{-1}$, example of calculation shown in Appendix B).

Table 4-4: TOC and HPLC values from after the adsorption phase compared in mg carbon per liter

Fe/MFI (no. experiments)	Average real TOC t=180 [mg/L]	Average paracetamol TOC t=180 [mg/L]	Difference TOC [mg/L]
30C (4)	53.6±2.5	44.1±2.2	9.5
45C (4)	55.1±1.6	48.3±1.5	6.8
60C (2)	56.8±1.6	51.9±4.2	4.9

The values in Table 4-4 are the average values with the standard deviation, calculated from at least two experiments. These results prove that there were other aqueous organic molecules than paracetamol, as the TOC values were higher than the calculated paracetamol TOC values. The standard deviation for the experiments at 60°C is too large to come to the same conclusion.

The occurring phenomena may have been degradation of the paracetamol, even though there was no H_2O_2 added. This might come from species in the solution with oxidation properties. Pignatello[24] proposed that the ferric ion produces hydrolyzed species (for instance $Fe(OH)_3$) when in contact with water, and although they are weak oxidants, they might oxidize the organic species to some extent[48]. Other possible degradations of the paracetamol molecule are; the rearrangement reaction as proposed by Ismail et al[34], where the acetyl group is relocated or cleaved off[23].

Figure 4-6 is the HPLC analysis showing the end of the adsorption phase for the Fe/MFI zeolite at 45°C, where two peaks are visible. The largest peak is the paracetamol, having a retention time of 8-8.2 minutes. The other peak (retention time of 6.3 minutes) usually appeared some time (1-10 minutes) after the zeolite was added (depending of the temperature), and increased slightly throughout the adsorption phase. This is a verification of the earlier mentioned pre-degradation occurring before the oxidation was started. The nature of this molecule is not known, but might be either a pre-oxidation product, or acid catalyzed cleavage product.

In Table 4-4 it is also possible to see an increase in the TOC differences with decreasing temperatures. An explanation for this could be an increasing degree of pre-oxidation due to; the higher amount of adsorbed organic molecules (due to the higher adsorption capacity at temperatures), implying that the pre-oxidation is proportional to the amount of physisorbed molecules, and not the aqueous concentration of the molecules. This would further imply that the pre-oxidation occurred mainly on physisorbed organic species.

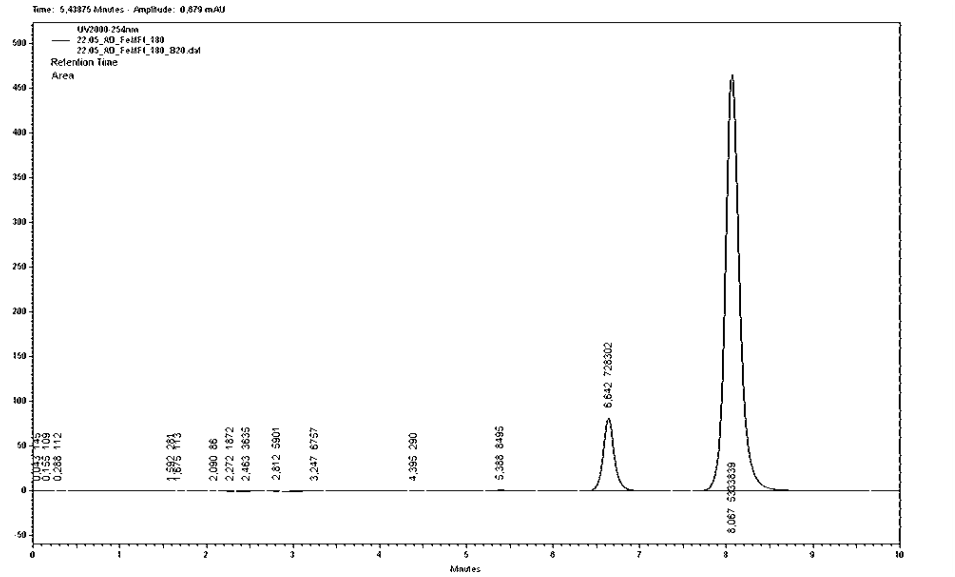

Figure 4-6: HPLC chromatogram after adsorption phase (180 min) with the Fe/MFI zeolite

4.2.2 Fe/BEA

The adsorption capacity of the Fe/BEA was superior to that of the Fe/MFI zeolite, probably since it had a superior specific surface area (see Table 3-3). It also performed a different trend in the converging part of the adsorption curve. The Fe/MFI induced a slow and continuous decrease in paracetamol concentration of the solution. In the presence of Fe/BEA, the paracetamol concentration showed first a steep decrease but finally increased until the end of the adsorption phase, see Figure 4-7.

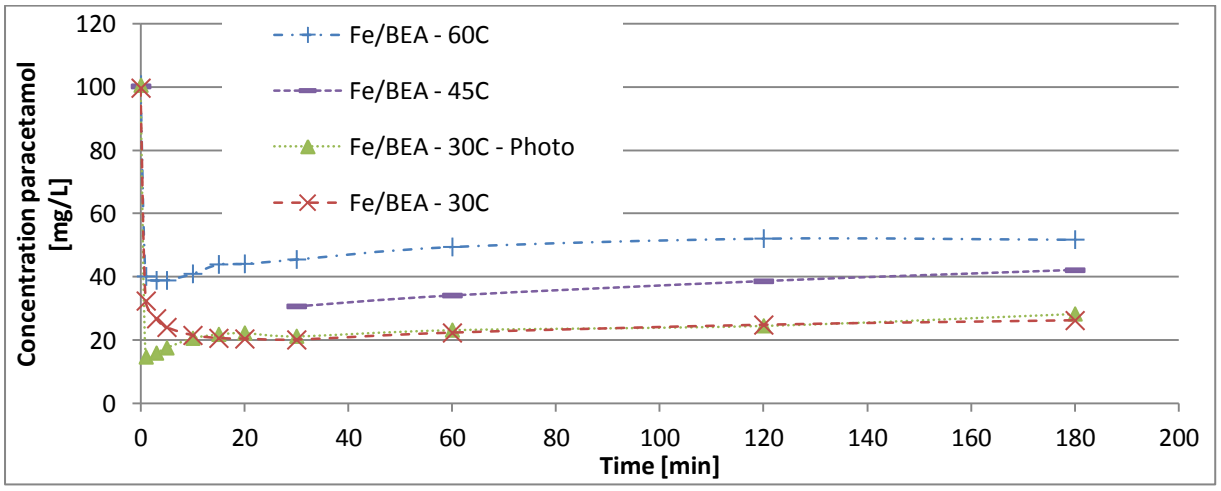

Figure 4-7: HPLC values for the adsorption of paracetamol on the Fe/BEA zeolite at temperatures: 30, 45 and 60°C

This increase of paracetamol concentration in the converging part could imply that there was competitive adsorption on the zeolite. This phenomenon could have occurred if the formed degradation products of paracetamol had a higher adsorption affinity than the paracetamol molecule itself. Since a degradation often leads to a cleavage of the organic molecules (for example the first step in the reaction mechanism of Figure 3-2), they could replace the paracetamol molecules in a higher rate than the paracetamol was being degraded, resulting in an increasing aqueous concentration of paracetamol, but a decrease in its overall concentration.

Table 4-5: TOC and HPLC values from after the adsorption phase compared in mg carbon per liter

Fe/BEA	Average real TOC t=180 [mg/L]	Average calc. paracetamol TOC t=180 [mg/L]	Difference TOC [mg/L]
30C (4)	24.0±2.4	17.9±0.8	6.1
45C (1)	33.1	26.9	6.2
60C (2)	40.3±0.2	33.4±0.5	6.9

A similar trend was also found for the Fe/BEA zeolite, where the calculated TOC values from the HPLC values were lower than the real TOC values. This difference was significant, as it was much larger than the calculated standard deviations. The unknown peak also appeared on the HPLC results with the Fe/BEA. This could have indicated that the paracetamol molecules were been degraded to some extent during the adsorption phase on Fe/BEA too. However the temperature dependency of the pre-oxidation could not be seen with Fe/BEA.

4.2.3 Competitive adsorption

On the addition of hydrogen peroxide to the reactor, the general trend was that the paracetamol concentration dropped rapidly, see Figure 4-2. The TOC values, on the other hand, often had a quick increase, like a step function, directly after the addition of the oxidant. One explanation for this could have been the competitive adsorption between the hydrogen peroxide and the adsorbed organic molecules on the zeolites, replacing the already adsorbed organic molecules. However the adsorption affinity of the oxidant was not investigated, so this was left as an assumption.

4.2.4 Adsorbed molecules

The amount of adsorbed organic molecules after the adsorption phase can be roughly estimated by assuming that no molecules were completely mineralized. By subtracting the TOC value from the end of the adsorption phase (t=180) from the initial TOC value (t=0). This difference should give an approximated amount of adsorbed organic molecules. This was proved for the adsorption Fe/MFI (last column in Figure 4-8), where the sum of liquid and solid carbon analyses equaled the liquid analysis before addition of zeolites.

For the adsorbed amount after the oxidation phase, the calculation may not be done in the same manner, as the amount of an adsorbed molecule is a function of the molecule's aqueous concentration. If there had been only one molecule in the solution, an isotherm could have been produced for the molecule in question, and the adsorbed amount could have been found, assuming instantaneous equilibrium. Yet in reality the solution contained a vast number of different molecules after the oxidation phase, with all molecules present in different concentrations and showing different adsorption affinities. Therefore the chosen method to determine the amount still adsorbed on the zeolite after the oxidation phase was to analyze the solid carbon content.

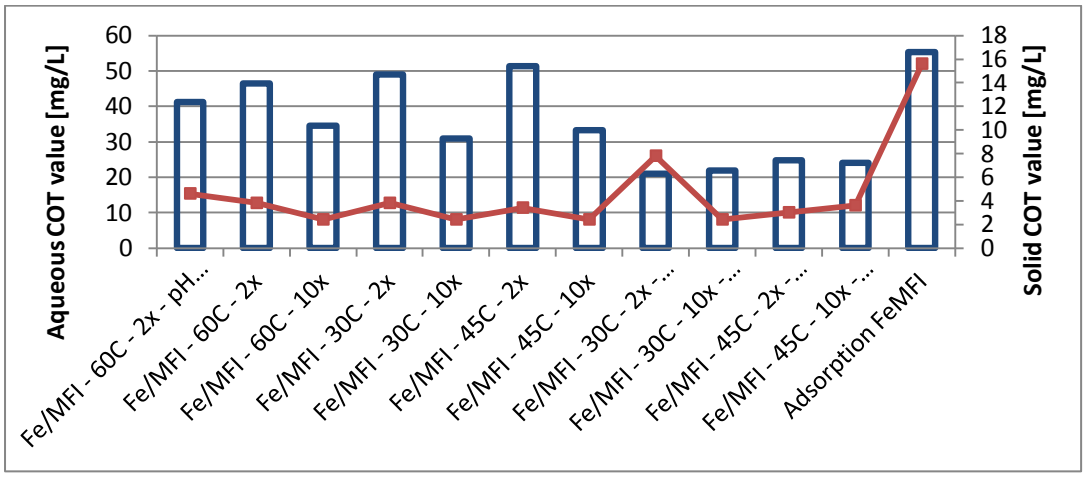

Figure 4-8: Aqueous COT values (blue columns) and solid carbon content (red points) after the oxidation phase (480 min)

The figure above show the results from the mentioned solid carbon analyses compared to the final TOC concentrations for all the Fe/MFI experiments. Excepting the photo-Fenton Fe/MFI experiment at 30°C and 2 times the stoechiometric concentration of oxidant and the adjusted pH, all carbon contents were very similar. This may have been caused by a long filtration time

as it was left overnight. This would have equilibrated the adsorption at an even lower temperature, obtaining a superior concentration of the solid carbon content compared to the final concentration. Another striking trend is that the values for the dark Fenton experiments are very similar for the experiments that have the same amount of oxidant, disregarding the actual aqueous concentration. It therefore seems that the amount of adsorbed pollutants at the end of the oxidation is neither dependent on temperature nor the aqueous pollutant concentration, but on the concentration of the oxidant.

4.2.5 Section summary

At the time of oxidant addition the adsorbed amount of paracetamol had not yet stabilized, but rather continued to slowly increase or decrease. This was explained by the degradation of the paracetamol molecule, and was proved partly by TOC and by qualitative HPLC. Even though the concentration of paracetamol was not completely stable after 180 minutes of adsorption, similar initial conditions for the oxidation phase were obtained for each temperature.

4.3 The Fenton reaction

In the previous section the adsorption phase was studied, and although there might have been other phenomena than the adsorption of paracetamol molecules, it was fairly straight forward. However in this section, the oxidation phase which has a far greater complexity than the adsorption phase will be investigated. The level of complexity is a result of the large number of different occurring events in the reactor, that all influence the measured values and each other. This first part will shortly describe the trends of the kinetics, without going too deep into the mechanism. To grasp the magnitude of it the following events will be taken into account:

A. The competitive physisorption between the oxidant and the organic molecules.
B. The oxidation of aqueous organic molecules by aqueous hydroxyl radicals.
C. The oxidation of physisorbed organic molecules by aqueous hydroxyl radicals.
D. The desorption of physisorbed organic molecules to equilibrate a decrease in aqueous organic molecules.

Table 4-6 was made to see how the different events probably would quantitatively affect the measured TOC value.

Table 4-6: Adsorption and reaction events occurring in the reactor and their effect on the TOC value

Event	Change in TOC value [-]	Consequence of the event
A	++	Oxidant replacing organic molecules
B	-	Some oxidation events lead to mineralization
C	+	One part stays adsorbed while the other migrates into the solution
D	+	Organic molecules migrating from solid to solution

As mentioned in section 2.3, the mechanism for the heterogeneous Fenton reaction is not known. Therefore it is not easy to determine which events have the superior magnitude. However knowing how the different events quantitatively would affect the reaction (table above) it is possible to study the reaction kinetics to see which events that may be dominant.

The plotted TOC values are presented with one standard deviation calculated using the Gaussian error propagation function with an error of 2% for the TOC apparatus and an error of 0.0001g for the sample preparation (formulas are presented in Appendix I).

4.3.1 Parameter dependency of the reaction kinetics with Fe/MFI

The paracetamol concentration was depleted within 180 minutes for the experiment at 30ºC and in less than 60 minutes for the experiments at 45 and 60ºC, for the two concentrations of oxidant.

An explanation of the three different TOC trends after the oxidant addition in Figure 4-9 could be the different reaction kinetics and adsorption affinities at each temperature for each species. At the lowest temperature (30°C) after adding the oxidant there was first a slight increase in TOC concentration (as seen in the enlarged image), possibly due to competitive physisorption with the oxidant. Where the kinetics of desorption of organic molecules were superior to that of the oxidation reaction (Event A>Event B).

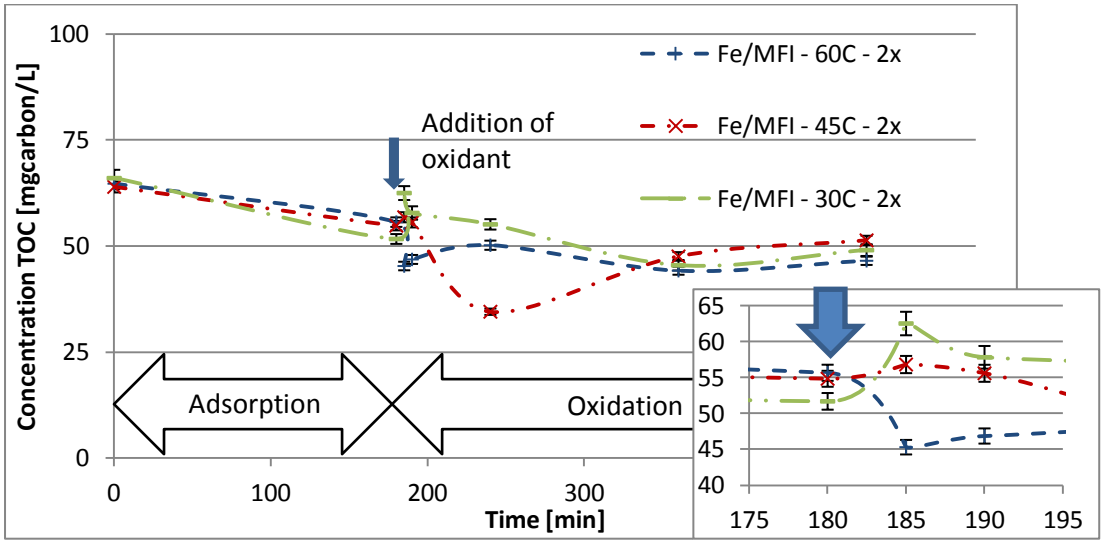

Figure 4-9: TOC values for the Fe/MFI experiments with 2x the stoechiometric oxidant at 30, 45 and 60ºC

However the trend for the highest temperature (60°C) was completely opposite, producing an initial drop in TOC concentration. Two explanations regarding the lower adsorption capacity at 60°C than at 30°C can explain this trend; a smaller amount of replaced organic molecules, and the kinetics of oxidation of the aqueous organic molecules would have been larger than the desorption kinetics (Event B>Event A). The other explanation is a lower amount of physisorbed oxidant (temporarily immobilized oxidant), leading to an instantly higher rate of mineralization, due to the higher production rate of hydroxyl radicals.

Both the curves for 30°C and 60°C followed the same trend after 240 minutes with a slow decrease of the TOC concentration. Safarzedeh-Amiri et al[17] explained this decreasing rate of mineralization for the homogeneous Fenton process by the formation of iron-carboxyl complexes inhibiting the iron catalyst. Another reason for the TOC value leveling out could be explained as desorption of organic molecules from the zeolites to the solution to equilibrate the aqueous mineralization (event D) and to migrate the mineralization product from the oxidation of adsorbed organic molecules (event C). So even though the TOC concentration seems to be constant or increasing the total organic carbon is decreasing (event D and C ~ event B).

Afterwards, looking at the experiment at 45°C the trend is different, as in has a smoother decrease in TOC concentration from the addition of the oxidant. This trend is surprisingly different to the trends obtained from the over and underlying temperatures. As the difference in the trends is mainly from one measurement with small systematic errors (t=240 min, 45°C), and that the experiment has not been repeated, it is probably caused by a random error, either during sampling or analyses. Further on, the trend for the experiment at 45°C follows that of the over and underlying temperatures.

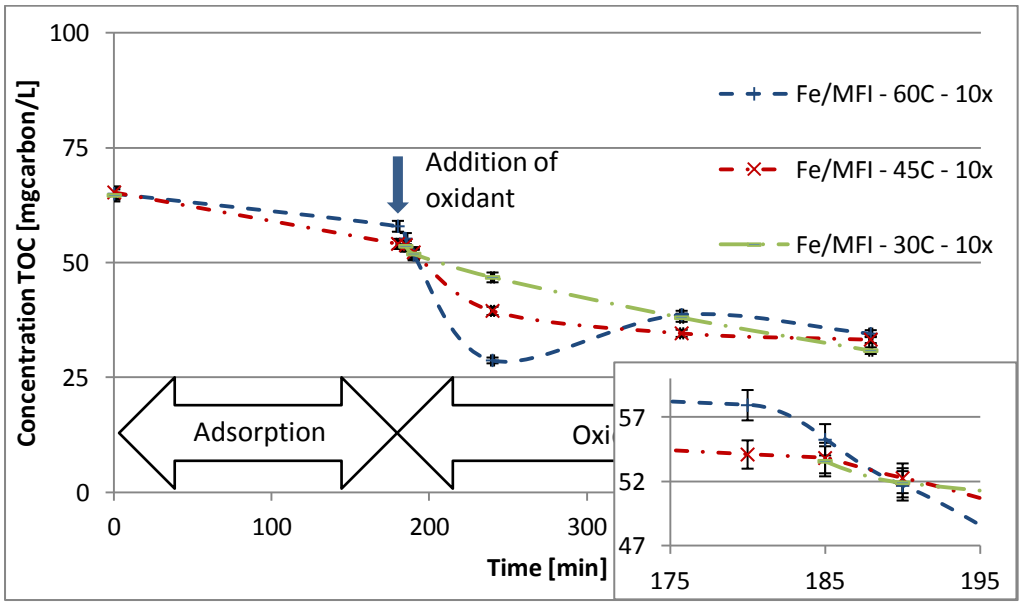

Figure 4-10: TOC values for the Fe/MFI experiments with 10x the stoechiometric oxidant at 30, 45 and 60°C

The TOC values presented in Figure 4-10 show a different dependency than for two times the stoechiometric concentration of oxidant. Here the three experiments follow more or less the

same trend, as can be seen from the overlapping standard deviations in all measurements but one (240min). The concentration decreases from the addition of the oxidant (Event B > Event C and D), and the magnitude of this decrease increases with increasing temperatures. The kinetic differences between the temperatures might be caused by augmented reaction rates with increasing temperature. In addition since the adsorption capacity decreased with increasing temperatures, the higher temperatures would have higher concentrations of oxidant and organic molecules, which in turn lead to a higher reaction rate. The result of this was that the higher temperature had a higher initial production rate of peroxide radicals, leading to; a high mineralization rate and a high rate of radical scavenging. The converging trend of the TOC concentrations could have been caused by the lowered aqueous concentration of oxidant and organic molecules, or the earlier mentioned catalyst inhibition by the carboxylate complexes.

4.3.2 Parameter dependency of the reaction kinetics with Fe/BEA

The experiments with the Fe/BEA catalyst showed faster paracetamol degradation than of the Fe/MFI catalyst was less than 180 minutes for the experiment at 30ºC and 5-10 minutes for the experiments at 45 and 60ºC.

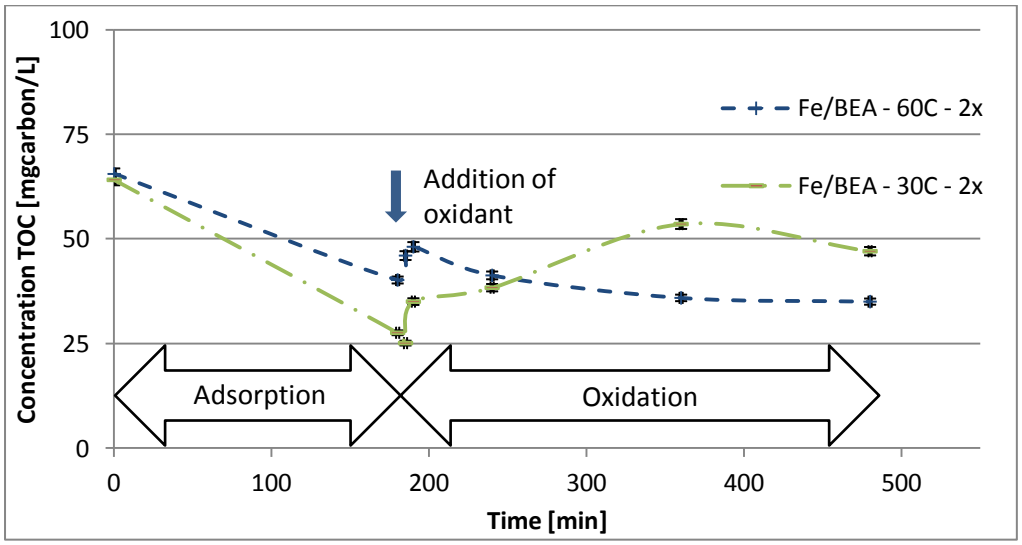

Figure 4-11: TOC values for the Fe/BEA experiments with 2x the stoechiometric oxidant at 30 and 60ºC

The trends found in Figure 4-11 are similar on addition of oxidant, as both of them have an immediate increase in TOC value. This was explained earlier as a competitive adsorption (as

for the Fe/MFI at 30°C and 2x oxidant) between the oxidant and the adsorbed organic molecules (Event A). It seems like this positive step in TOC concentration occurs when the adsorption capacity is high; Fe/MFI at low temperature, or Fe/BEA which has a superior specific adsorption area (50% larger than the Fe/MFI).

After this the trends differed; the experiment at the highest temperature had a continuous decreasing degradation leveling out at the end of the oxidation phase, ending up at a TOC value lower than for the other temperature. The plottet TOC values are also clearly separated, meaning the large difference in trend were rather cause by random than systematic errors. The diminishing reaction rate is probably caused by the chelating organic intermediates (iron-carboxyl complexes).

Remembering that the highest temperature also has the weakest adsorption capacity (underestimating its degree of mineralization) proves that the Fe/BEA had an even greater difference in the degree of mineralization at high temperatures than at low temperatures, than what is presented in the figure.

The explanation for the trend of the lower temperature could have been a lower rate of mineralization of the aqueous organic molecules (event B) than of the adsorbed organic molecules (event C). This resulted in liberation of the oxidation products from the zeolite, increasing the aqueous TOC concentration, while decreasing the total TOC concentration. The lower aqueous concentration caused by higher adsorption capacities at lower temperatures, would lead to a lower reaction rate, enforcing this assumption.

Similar trends were found for the experiments with Fe/BEA at ten times the stoechiometry of oxidant.

4.3.3 Different kinetics by introduction of the UV-irradiation

The photo-Fenton experiments were performed with the same conditions as for the dark Fenton experiments, only difference was the addition of the UV-irradiation. The paracetamol degradation was less than 180 minutes for the experiment at 30ºC and less than 60 minutes for the experiment at 45ºC. The TOC concentrations from the experiments at 30°C are presented in Figure 4-12 and the results from the experiments at 45°C were not added as they showed similar trends.

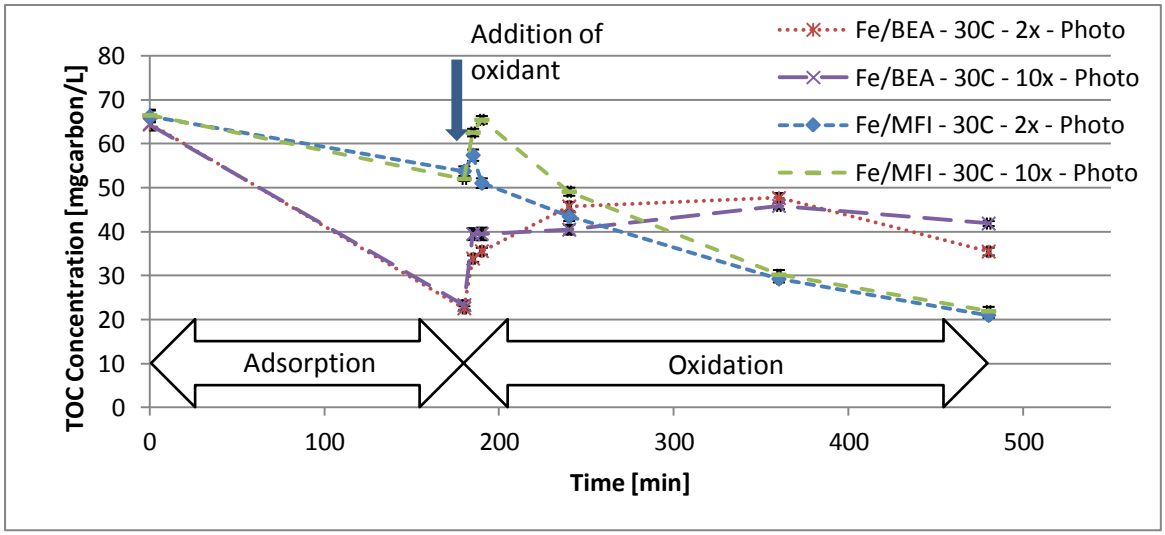

Figure 4-12: TOC values for the photo-Fenton experiments at 30°C at the 2x and 10x the stoechiometric oxidant for the Fe/MFI and the Fe/BEA zeolite

A similar trend for both the catalysts can be seen, in that after addition of the oxidant TOC concentration increased, the TOC concentration increase was also larger for the higher oxidant concentration in both cases. This was probably due to the earlier explained competitive adsorption (Event A). Other than this difference after the addition of oxidant, the trends are very similar statistically as can be seen from the overlapping error bars.

The major difference in the kinetics of the process can be seen for the experiments with the Fe/MFI, that actually have a continuing mineralization after 300 minutes of oxidation. The reason for this is probably that the formed iron-carboxyl complexes are destroyed by the UV-irradiation, liberating trapped iron catalyst, as shown in Eq.(2.12). However it is not known if this only applies to the leached iron or if it also is applicable to the solid iron. The amount of leached iron, as will be presented later was in general smaller for the photo-Fenton than for the dark-Fenton, two-five times smaller for the Fe/MFI experiments and about ten times smaller for the Fe/BEA catalyst.

The photo-Fenton experiments with Fe/BEA show similar trends as in the dark Fenton reaction at 30ºC, with a slightly improved TOC conversion for the photo-Fenton experiments.

4.3.4 Degree of mineralization depending on the oxidant concentration

The calculation of the TOC conversion is shown in section 4.1.3 using the initial and final TOC value. The concentration of the oxidant was investigated at 2 and 10 times the necessary stoechiometry of the complete mineralization equation for paracetamol (calculated in Appendix C).

The plotted values in Figure 4-13 give a clear picture of how the TOC conversions were affected by the two concentrations of the oxidant. The experiments with Fe/MFI showed a higher degree of mineralization for the larger oxidant concentration. By looking at the standard deviation for these values, the TOC conversions were fairly similar implying that the TOC conversion had little temperature dependency at the highest oxidant concentration. The Fe/BEA experiments showed an exactly opposite trend and had a clear dependency of the temperature.

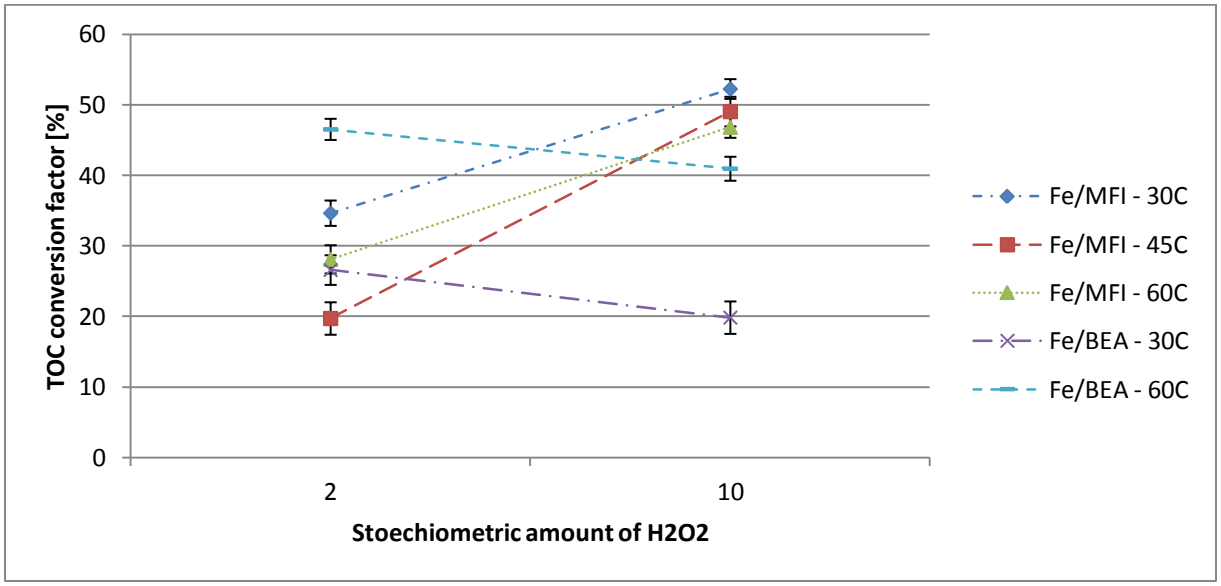

Figure 4-13: TOC conversions for the dark-Fenton experiments at the two different oxidant concentrations

As indicated from the reaction rates of Walling[15], for each temperature, nature and concentration of the iron source, there is an optimum oxidant concentration with respect to the kinetics. Inferior to this concentration the hydroxyl radical is not produced in sufficient quantities to give a high degree of mineralization. On the other hand, superior to it, the production of the radical is too high, leading to high rates for the scavenging reactions. The exact position of the optimum oxidant concentration is difficult to predict, but it is probably less than ten times the stoechiometry for the Fe/BEA zeolite, more than two times for the Fe/MFI zeolite, concluding from Figure 4-13.

On the other hand, there is also an optimal oxidant concentration regarding the degree of mineralization, at which the oxidant is used most efficiently. This is not the same point as for the formerly explained optimum, and it will be close to the lower oxidant concentration for

both the catalysts. And as will be explained in section 4.5 the oxidant is more efficiently used by the Fe/BEA catalyst than the Fe/MFI catalyst.

4.3.5 Fenton – photo-Fenton

The comparison between the Fenton experiments and the photo-Fenton experiments were done to see if the UV-irradiation had an effect on the conversion or not. Looking at the equations for the photo-Fenton in section 2.4, logically it should give a higher yield as the UV-irradiation contributes with an independent production of hydroxyl radicals and regeneration of the catalyst. The destruction of the iron-carboxyl complexes also favors the increased rate of mineralization when going from dark to photo-Fenton, as this complexation is one of the reasons the dark-Fenton has a decreasing reaction rate towards the end.

Figure 4-14 shows a plot of the degrees of mineralization for the experiments with and without irradiation and as can be seen; the experiments with the UV-irradiation always exhibit a larger conversion than in the dark experiments.

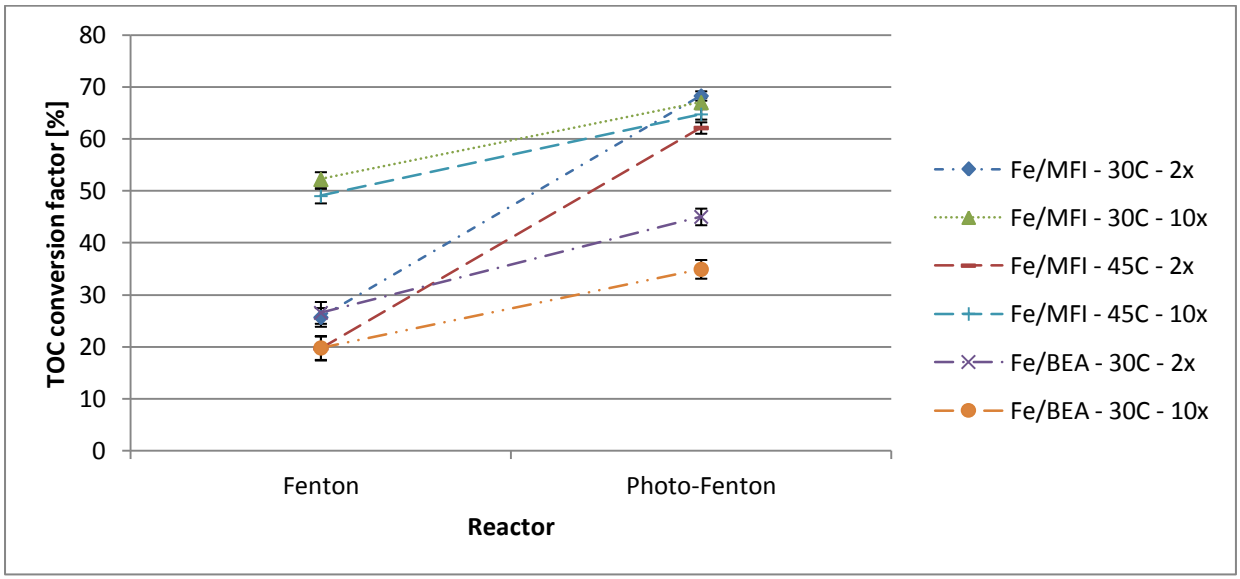

Figure 4-14: TOC conversions from the dark-Fenton reactor compared to the photo-Fenton reactor

The experiments that had the highest degrees of mineralization were all the Fe/MFI experiments with UV-irradiation. Figure 4-14 also shows a remarkably similar increase in mineralization for the experiments done at the same oxidant concentrations. This implies that the additional effect of the UV-irradiation mostly depended on the oxidant concentration.

Interestingly the dependency upon the oxidant concentration for the experiments with the Fe/MFI zeolites almost vanished by introducing UV-irradiation. This was caused by the dramatic increase in degree of mineralization for the smallest oxidant concentration in going from "dark-" to photo-Fenton, while only a slight increase for the higher oxidant concentration.

The Fe/BEA on the other still maintained the higher degree of mineralization for the lower oxidant concentration.

4.4 Highest degree of mineralization

The most important goal in this study was to reduce the organic content of the reactor. In Table 4-7 the TOC conversions for every experiment with standard deviations are listed (the standard deviations are calculated as in Appendix I with the Gaussian error propagation formula from the maximum allowed standard deviation from the TOC-apparatus of 2%). The true TOC conversion is not noted with their standard deviation, as the solid TOC analyses were performed at another institution and they could not be obtained.

Table 4-7: Liquid and liquid + solid based TOC conversions for all the conducted experiments

Reactor	TOC conversion [%]	True TOC conversion (sol.+liq.) [%]
Fe/MFI - 30C - 2x - photo	68.3±0.9	56.5
Fe/MFI - 30C - 10x - photo	67.0±0.9	63.4
Fe/MFI - 45C - 10x - photo	64.8±1.0	59.5
Fe/MFI - 45C - 2x - photo	62.2±1.1	57.6
Fe/MFI - 30C - 10x	52.3±1.4	48.5
Fe/MFI - 45C - 10x	49.0±1.4	45.4
Fe/BEA - 60C - 2x - pH = 2.8	47.5±1.5	
Fe/MFI - 60C - 10x	46.8±1.5	43.1
Fe/BEA - 60C - 2x	46.5±1.5	
Fe/BEA - 30C - 2x - photo	45.0±1.6	
Fe/BEA - 60C - 10x	41.0±1.7	
Fe/BEA - 30C - 10x - Photo	35.0±1.8	
Fe/MFI - 60C - 2x - pH = 2.8	33.2±1.9	
Fe/MFI - 60C - 2x	28.1±2.0	22.2
Fe/BEA - 30C - 2x	26.6±2.1	
Fe/MFI - 30C - 2x	25.7±1.8	20.0
Fe/BEA - 45C - 10x	25.3±2.1	
Fe/BEA - 30C - 10x	19.8±2.3	
Fe/MFI - 45C - 2x	19.7±2.3	14.4

The highest degrees of mineralization achieved were only slightly lower as those found in 2011 by Duran[7] and Almeida[27], who obtained 71.5% in the continuous homogeneous photo-Fenton process and 75% in the solar-electro-Fenton process respectively. However it is worth mentioning that the heterogeneous photo-Fenton has several advantages to these two processes with respect to complexity and catalyst recycling. It was also seen that among these best results showed little dependency on the oxidant concentration and the temperature.

When including the results from the solid carbon content to the calculation of the liquid TOC the (true TOC conversion) value is slightly lower (~5%), but the best results are still significantly better than the minimum necessary conversion (≥18%) proposed by Jordá et al in 2011 to achieve a sufficient biodegradability of the pollutants[32]. The solid carbon content was not analyzed for the Fe/BEA as it was not performing as well as the Fe/MFI. The TOC conversion would however be at least five percent lower than the listed values, as the Fe/BEA had a significantly higher adsorption area.

The dark Fenton Fe/MFI experiments achieved TOC conversions in the same range for a given oxidant concentration (shaded in Table 4-7), regardless of temperature. This was also seem earlier when studying the kinetics, and leads to the conclusion that the TOC conversions of the experiments with the Fe/MFI zeolite have a higher dependency of the oxidant concentration than for the temperature.

4.5 Other aspects

The other objective was to select the best catalysts for subsequent continuous experiments, as presented analyses had so far given promising results. As can be seen from Figure 4-15, there was a clear tendency for the two catalysts during the experiments. The Fe/BEA had a significantly larger leached iron concentration, which was no good property regarding the continuous process. This larger concentration was probably due to a higher amount of organic acids in the Fe/BEA experiments, complexating the solubilized iron, as proposed by Johnson et al[49] in 1997; organic chelatants increases the Fe solubility in seawater.

These higher leached iron concentrations led to a high mineralization yield for the Fe/BEA leachate experiments than for the Fe/MFI experiments. This might be explained from the nature of the iron ions, as a high amount of ferric ions give a very low contribution to the production of hydroxyl radicals.

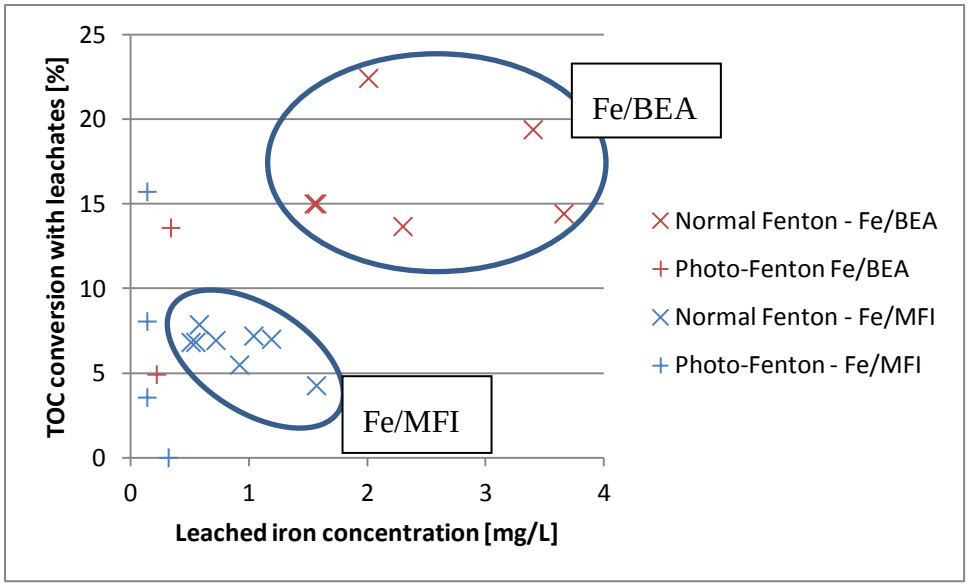

Figure 4-15: The leachate TOC conversion as a function of the leached iron concentration

The photo-Fenton reactor experiments had lower leached iron amounts than the dark Fenton experiments. This was probably due to the fact that the UV-irradiation breaks up the iron-carboxyl complexes[17], avoiding the earlier mentioned increased Fe-solubility.

Even though the Fe/MFI produced the best degrees of mineralization, it also involved a high consumption of oxidant. Regardless of the initial concentration of oxidant it was nearly consumed in every experiment.

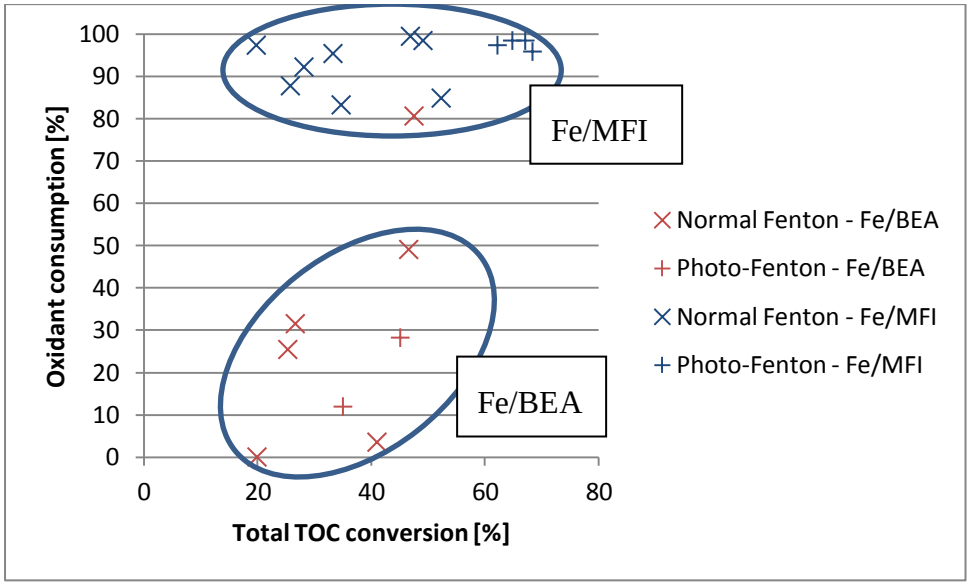

Figure 4-16: The effectiveness of the experiments, oxidant consumption versus TOC conversion

The higher consumption of oxidant was a result of the differing oxidant scavenging properties of the two zeolites. The combination of a slightly higher iron concentration and smaller crystallites in the Fe/MFI, both leading to a larger number of active sites could have lead to the higher degree of scavenging.

Although the Fe/MFI consumes a much higher amount of oxidant, the choice of the photo-Fenton oxidation with Fe/MFI and two times the stoechiometry of oxidant would probably be the best choice. If a UV-lamp is not available, the same catalyst and temperature should be chosen, but with a higher concentration of oxidant.

4.6 Intermediates

The possible intermediates produced from a Fenton oxidation were presented in section 3.1.2, with the conclusion that the Fenton process ends up with a mixture that has less toxicity and which is more biodegradable than the initial paracetamol containing solution. As earlier mentioned in section 3.6.1, the individual species identification with the HPLC is a troublesome work, and by using the fast analysis method that was applied to validate the kinetics of the paracetamol degradation, it is nearby impossible to distinguish the different peaks (see Figure F-1). In addition, not all the intermediates are visible at the two chosen wavelengths. Another method was applied to separate the peaks better; HPLC-Mass Spectroscopy (HPLC-MS). This method uses the principle of chromatography to separate the individual compounds, and furthermore uses the exact weight to identify them. The reaction solution from one Fe/MFI experiment was analyzed, and individual peaks were detected. The main intermediates found were:

- Acetic acid
- Acetamid
- Maleic acid
- Two unidentified peaks were also found
- No aromatics were detected

The acetamid and the maleic acid correspond to the intermediates proposed by Almeida et al[27], signifying that a similar degradation mechanism had been followed. The acetamide might pose a problem as it is cancerogeneous. The nature of the two unidentified peaks will also

have an impact on the total biodegradability and the toxicity of the reaction mixture. They will be identified during the future work on this topic.

5 Conclusion

The effects of H_2O_2 concentration and temperature on the heterogeneous Fenton oxidation of water containing paracetamol have been investigated. Applied catalysts were commercial iron-doped zeolites, ZSM-5 (Fe/MFI) and Beta (Fe/BEA). The photo-Fenton (medium pressure mercury vapor lamp) has also been investigated.

The iron doped zeolites have proven to be efficient for the photo-Fenton process achieving TOC conversion up to 70% after five hours of oxidation, which is similar to the highest degrees found literature regarding the treatment of water polluted by paracetamol.

The Fe/MFI catalyst gave the highest degrees of mineralization, after five hours of oxidation, based on the liquid phase (68%) in the photo-Fenton experiment at 30ºC and two times the stoechiometric amount of oxidant for full mineralization. When including the solid carbon content the degree of mineralization was 5-10% lower for each experiment. The Fe/MFI in general had the lowest amount of leached iron (<3.2% loss of iron catalyst) and the lowest activity of this leached iron. The downside was that it had a superior consumption of oxidant to the Fe/BEA.

The Fe/BEA catalyst on the other hand had a poorer performance with degrees of mineralization based on the liquid phase less than 50% in five hours of oxidation. Best performance for the Fenton experiment at 60ºC, two times the amount of oxidant and an initial adjusted pH at 2.8. The experiments with the Fe/BEA also led to a higher amount of leached iron (<5.9% loss of iron catalyst). The solid carbon content was not analyzed the Fe/BEA experiments, so the TOC conversions were only based on the liquid phase

With respect to the kinetics of the heterogeneous Fenton process there were three major events occurring in the reactor. The **first** event was the oxidation of organic molecules. A complex case as the reaction mechanism is not yet fully understood. In addition the zeolites have a large capacity of physisorption, dividing the event into oxidation of *aqueous **and** adsorbed* organic molecules. The **second** event was desorption of organic molecules from the zeolite surface, which continuously increases the aqueous (measured) organic content in solution. The **third** event is the deactivation of the iron catalyst by formation of complexes with the intermediates. This continuously decreases the rate of the reaction for the dark-Fenton processes. In the photo-Fenton process however, the rate does not decrease in the same manner, as the complexes are destroyed by the UV-irradiation. It is assumed that this

complex irradiation also lead to a lower leached iron content for the photo-Fenton experiments.

All the aromatics are successfully removed during the process and the final organic products from the process have a higher biodegradability and in general a lower toxicity than the initial paracetamol molecule.

6 Further recommendations

It would be interesting to investigate the recycling or the continuous use of the catalyst, as this is one of the major advantages of the heterogeneous process compared to the homogeneous process. The experiments should study both the activity and the loss of catalyst.

Another interesting study is to investigate several catalyst concentrations to see if a higher degree of mineralization may be obtained.

To better understand the kinetics, the experiments could be run in a different manner. Instead of taking five samples during the reaction, five separate experiments can be run, that are completely quenched at each sample time respectively. This would enable a study of the kinetics of the adsorbed molecules to obtain the real carbon conversion, the nature of the intermediates and the leached iron.

A comparison of the intermediates produced with the two catalysts would be interesting, as it might be the reason for the higher leachate concentration and activity for the Fe/BEA than for the Fe/MFI.

7 References

1. B. Halling-Sorensen, S. N. Nielsen, P. F. Lanzky, F. Ingerslev, H. C. H. Lutzhoft and S. E. Jorgensen, *Chemosphere*, 1998, **36**, 357-394.
2. K. Fent, A. A. Weston and D. Caminada, *Aquat Toxicol*, 2006, **76**, 122-159.
3. T. A. Ternes, *Water Research*, 1998, **32**, 3245-3260.
4. L. Parisien, Le paracétamol en tête, http://www.leparisien.fr/societe/le-paracetamol-en-tete-02-07-2007-2008173740.php, Accessed 13th of July, 2012.
5. P. H. Roberts and K. V. Thomas, *Sci Total Environ*, 2006, **356**, 143-153.
6. M. Grung, T. Källqvist, S. Sakshaug, S. Skurtveit and K. V. Thomas, *Ecotox Environ Safe*, 2008, **71**, 328-340.
7. A. Duran, J. M. Monteagudo, A. Carnicer and M. Ruiz-Murillo, *Desalination*, 2011, **270**, 124-129.
8. H. J. H. Fenton, *Journal of the Chemical Society*, 1894, **65**, 899-910.
9. F. Haber and J. Weiss, *Proceedings of the Royal Society of London. Series A, Mathematical and Physical Sciences*, 1934, **147**, 332-351.
10. H. Zhang, H. J. Choi and C.-P. Huang, *Journal of Hazardous Materials*, 2005, **125**, 166-174.
11. C. P. Huang, C. Dong and Z. Tang, *Waste Management*, 1993, **13**, 361-377.
12. W. H. Glaze, J.-W. Kang and D. H. Chapin, *Ozone: Science & Engineering*, 1987, **9**, 335-352.
13. W. M. Haynes and D. R. Lide, *CRC Handbook of Chemistry and Physics: A Ready-Reference Book of Chemical and Physical Data*, Taylor & Francis Group, 2010.
14. G. Centi, S. Perathoner, T. Torre and M. G. Verduna, *Catalysis Today*, 2000, **55**, 61-69.
15. C. Walling, *Accounts Chem Res*, 1975, **8**, 125-131.
16. O. Garcia-Rojas, C. Gomez-Quitero, M. Rios-Bolivar, A. Romero and A. Rodriguez, *Adv Intell Soft Comp*, 2012, 251-258.
17. A. Safarzadeh-Amiri, J. R. Bolton and S. R. Cater, *Water Research*, 1997, **31**, 787-798.
18. A. Goti and F. Cardona, eds. P. Tundo and V. Esposito, Springer Netherlands, 2008, pp. 191-212.
19. J. Yoon, Y. Lee and S. Kim, *Water Sci Technol*, 2001, **44**, 15-21.
20. M. Dükkancı, G. Gündüz, S. Yılmaz and R. V. Prihod'ko, *Journal of Hazardous Materials*, 2010, **181**, 343-350.
21. M. B. Kasiri, H. Aleboyeh and A. Aleboyeh, *Appl Catal B-Environ*, 2008, **84**, 9-15.
22. T. L. P. Dantas, V. P. Mendonça, H. J. José, A. E. Rodrigues and R. F. P. M. Moreira, *Chem Eng J*, 2006, **118**, 77-82.
23. J. Feng, X. Hu, P. L. Yue, H. Y. Zhu and G. Q. Lu, *Chemical Engineering Science*, 2003, **58**, 679-685.
24. J. J. Pignatello, D. Liu and P. Huston, *Environ Sci Technol*, 1999, **33**, 1832-1839.
25. K. P. Henschel, A. Wenzel, M. Diedrich and A. Fliedner, *Regulatory Toxicology and Pharmacology*, 1997, **25**, 220-225.
26. R. Andreozzi, V. Caprio, R. Marotta and D. Vogna, *Water Research*, 2003, **37**, 993-1004.
27. L. C. Almeida, S. Garcia-Segura, N. Bocchi and E. Brillas, *Appl Catal B-Environ*, 2011, **103**, 21-30.
28. M. D. G. De Luna, M. L. Veciana, C.-C. Su and M.-C. Lu, *Journal of Hazardous Materials*, 2012, **217–218**, 200-207.
29. Sciencelab, MSDS for Oxalic acid, www.sciencelab.com/msds, Accessed 24th of June, 2012.

30. A. Sharma, A. Kumar, A. Kapoor, R. Kumar, S. V. Gangal, V. Gangal and S. D. Makhijani, *Bulletin of Environmental Contamination and Toxicology*, 1996, **57**, 34-40.

31. Sciencelab, MSDS for Acetamide, www.sciencelab.com/msds, Accessed 12th of July, 2012.

32. L. S.-J. Jordá, M. M. B. Martín, E. O. Gómez, A. C. Reina, I. M. R. Sánchez, J. L. C. López and J. a. S. Pérez, *Journal of Hazardous Materials*, 2011, **186**, 1924-1929.

33. J. Čejka and H. Van Bekkum, *Zeolites and Ordered Mesoporous Materials: Progress and Prospects : the 1st FEZA School on Zeolites, Prague, Czech Republic, August 20-21, 2005*, Elsevier, 2005.

34. R. Ismail, P. Adryan and F. Roessner, *Jordan Journal of Chemistry*, 2007, **2**, 235-245.

35. C. Baerlocher, L. B. Mccusker, D. Olson and I. Z. a. S. Commission, *Atlas of Zeolite Framework Types*, Elsevier, 2007.

36. M. H. W. Sonnemans, C. Denheijer and M. Crocker, *J Phys Chem-Us*, 1993, **97**, 440-445.

37. S. M. Csicsery, *Abstr Pap Am Chem S*, 1983, **185**, 44-Fuel.

38. J. Weitkamp, *Solid State Ionics*, 2000, **131**, 175-188.

39. G. T. Kokotailo, S. L. Lawton, D. H. Olson, D. H. Olson and W. M. Meier, *Nature*, 1978, **272**, 437-438.

40. A. Martucci, L. Pasti, N. Marchetti, A. Cavazzini, F. Dondi and A. Alberti, *Microporous and Mesoporous Materials*, 2012, **148**, 174-183.

41. J. C. Jansen, E. J. Creyghton, S. L. Njo, H. Vankoningsveld and H. Vanbekkum, *Catalysis Today*, 1997, **38**, 205-212.

42. M. Haddou, *Dégradation de dérivés de l'acide benzoïque par les procédés d'oxydation avancée en phase homogène et hétérogène: procédés Fenton, photo-Fenton et photocatalyse*, 2010.

43. F. Rouessac and A. Rouessac, *Chemical Analysis: Modern Instrumentation Methods And Techniques*, John Wiley & Sons, 2007.

44. E. R. Kuhn, *Lc Gc N Am*, 2002, **20**, 474-+.

45. N. Kambia, A. Luyckx, T. Dine, T. Dupin-Spriet, B. Gressier and C. Brunet, *Eur. J. Pharm. Sci.*, 2006, **12**, 81-84.

46. P. Bautista, A. F. Mohedano, J. A. Casas, J. A. Zazo and J. J. Rodriguez, *Journal of Chemical Technology & Biotechnology*, 2008, **83**, 1323-1338.

47. D. H. Everett, *Pure Appl Chem*, 1972, **31**, 577-638.

48. B. L. Railsback, Some Fundamentals of Mineralogy and Geochemistry, http://www.gly.uga.edu/railsback/FundamentalsIndex.html, Accessed 27.06, 2012.

49. K. S. Johnson, R. M. Gordon and K. H. Coale, *Marine Chemistry*, 1997, **57**, 137-161.

50. Q. Peñate, Doctorat, Université de Toulouse, 2009.

51. G. H. Aylward and T. J. V. Findlay, *SI Chemical Data*, John Wiley & Sons Australia, 2007.

52. H. A. Jakobsen, *Chemical Reactor Modeling: Multiphase Reactive Flows*, Springer, 2008.

Appendix A Calibration curves for HPLC

Two different HPLC apparatus were used in this work, and calibration curves were calculated for both of them. The samples for the HPLC ranged from zero to one hundred milligrams per liter, therefore five calibration samples within this region were introduced into the HPLCs. The areas obtained from the HPLCs are listed in Table A-1.

Table A-1: Concentrations of the calibration of the HPLC apparatus and their obtained areas

Concentration [mg/L]	Area Spectra system [-]	Area Varian [-]
5.0212	389120.5	184388
19.8944	1500666.5	632896
39.8586	2958466	1235586
69.8048	5197616	2131116
100.1000	7362856	2893400

These values were plotted in Excel and the equations for the calibration curves were found by regression, see Figure A-1. An assumption was made that a paracetamol concentration equal to zero would give an area of zero as well. Mathematically the regression curve was forced through the origin and a satisfying value for r-squared was obtained.

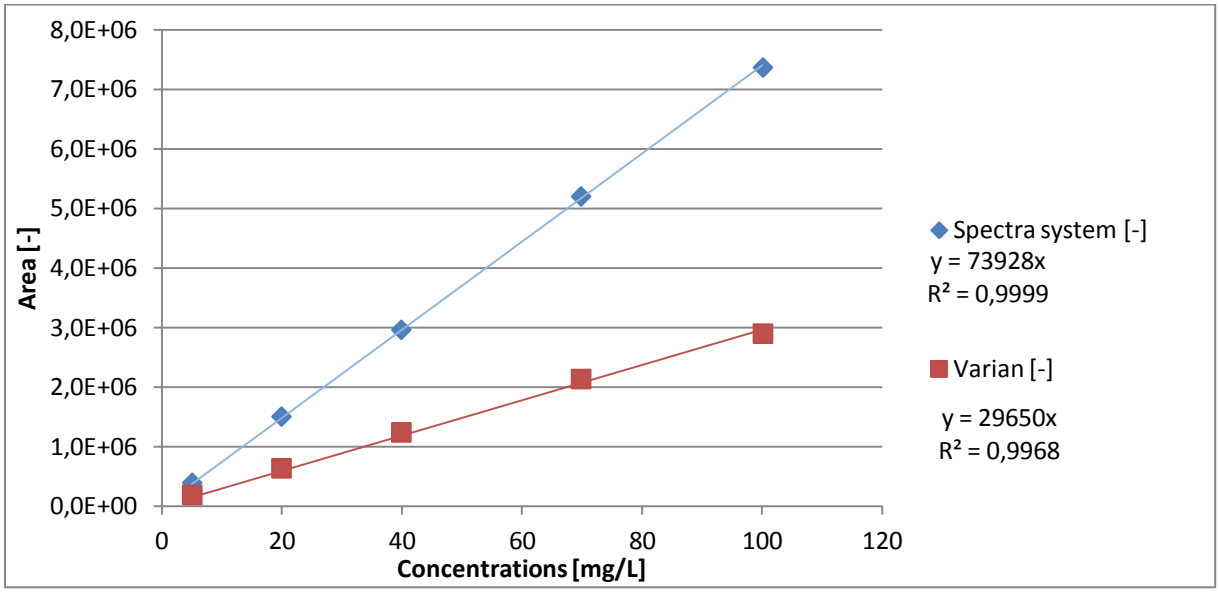

Figure A-1: Calibration curves for HPLC, area obtained as a function of the paracetamol concentration

The post analysis calculations for every sample analyzed, was dividing the resulting area with the slope of the calibration curve.

Appendix B Calibration curves for TOC

The samples for the TOC analyses were diluted two times; first they were diluted by a factor of six to eight (6/8) when they were mixed with the inhibitor solution, and afterwards by a factor of eight to twenty four (8/24) when they were diluted with ultra pure water. The maximum concentration of paracetamol was 100mgL^{-1}, with dilutions and conversion from mg paracetamol to mg carbon the maximum TOC concentration is calculated:.

$$C_{TOC}^{\max} = 100[mg/L] \cdot \frac{6}{8} \cdot \frac{8}{24} \cdot \frac{8[Carbon/Paracetamol \cdot]12[mg/mmol]}{150{,}16[mg/mmol]} \approx \underline{16\,mg/L}$$

Zero to one hundred milligrams paracetamol per liter equals: zero to sixteen milligrams carbon per liter. A 10% bigger safety interval was chosen. Seven calibration samples from paracetamol were inserted into the TOC that handed back the area obtained, see Table B-1.

Table B-1: Concentrations of the calibration samples for the TOC apparatus and their obtained areas

Concentration [mg/L]	Area 1 [-]	Area 2 [-]	Average area [-]
0.8137	6.88	6.98	**6.93**
1.5875	10.66	10.58	**10.62**
3.9744	24.60	24.42	**24.51**
8.0351	49.60	49.46	**49.53**
11.7977	71.25	71.08	**71.17**
13.9215	85.22	84.54	**84.88**
17.8974	108.20	108.00	**108.10**

The concentrations were plotted against the average areas, and a regression gave the equation for the calibration curve, see Figure B-1.

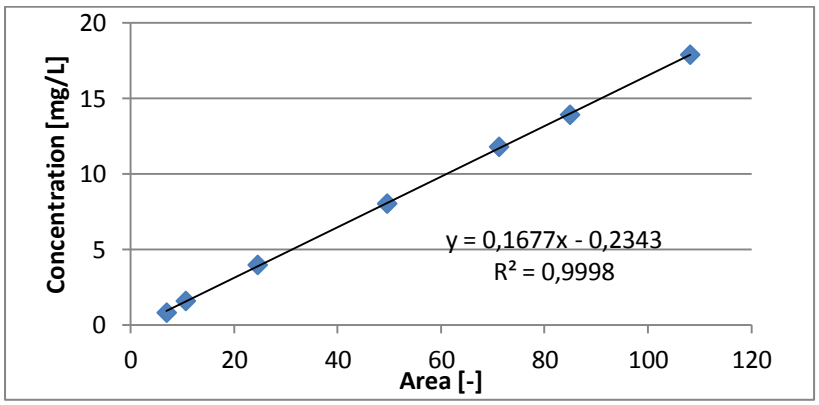

Figure B-1: Calibration curve TOC, carbon concentration as a function of the area obtained

Concentration values were obtained by inserting the obtained area into the equation obtained as x.

Appendix C Stoechiometric calculations H_2O_2

The stoechiometric amount of oxidant needed in the reactor was found using the complete mineralization equation as presented by Peñate et al[50].

$$C_8H_9NO_2 + 21H_2O_2 \rightarrow 8CO_2 + HNO_3 + 25H_2O$$

According to this equation, 21 molecules of oxidant were needed to mineralize one paracetamol molecule. The molar concentration of paracetamol in the solution:

$$C_{n,paracetamol} = \frac{C_{m,paracetamol}}{M_{paracetamol}} = \frac{100\,{}^{mg}/_{L}}{151.17\,{}^{mg}/_{mmol}} = \underline{0.66\,{}^{mmol}/_{L}}$$

The oxidant had a concentration of 30wt% H_2O_2 with a density of 1100mgmL^{-1}, while the molecular weight of H_2O_2 is 34.02mgmmol^{-1}. The stoechiometric amount of oxidant was calculated:

$$V_{H_2O_2} = \frac{21 \cdot C_{n,paracetamol} \cdot M_{H_2O_2}}{C_{H_2O_2 in 30\%H_2O_2} \cdot \rho_{30\%H_2O_2}} =$$

$$\frac{21\,{}^{mmolH_2O_2}/_{mmolparac.} \cdot 0.66\,{}^{mmolparac.}/_{L} \cdot 34.02\,{}^{mgH_2O_2}/_{mmolH_2O_2}}{0.30\,{}^{mgH_2O_2}/_{mg30\%H_2O_2} \cdot 1100\,{}^{mg30\%H_2O_2}/_{mL30\%H_2O_2}} \approx \underline{1.43\,{}^{mL}/_{L}}$$

The stoechiometric hydrogen peroxide for a total mineralization of a 100 mgL^{-1} paracetamol solution is 1.43mLL^{-1}.

Appendix D Standardization of the $KMnO_4$ solution

For every titration of H_2O_2 the titrant, potassium permanganate, has to be standardized to know its exact concentration. This is done by titrating it against a know amount of potassium oxalate, $K_2C_2O_4$, in acidic conditions (using conc. H_2SO_4).

$$2MnO_4^-(aq) + 5C_2O_4^{2-}(aq) + 16H^+(aq) \rightarrow 10CO_2(g) + 2Mn^{2+}(aq) + 8H_2O(l)$$

The concentration of the permanganate solution is further found by calculating the amount of consumed permanganate at equilibrium, at the first permanent color change of the solution.

$$C_{KMnO_4} = \frac{C_{C_2O_4^{2-}} \cdot V_{C_2O_4^{2-}}}{V_{KMnO_4}} = \frac{m_{K_2C_2O_4}}{M_{K_2C_2O_4} \cdot V_{KMnO_4}}$$

An example calculation of standardization is given in Table D-1.

Table D-1: Values from the standardization of the potassium permanganate solution with potassium oxalate

$K_2C_2O_4$, m_1	0.05	g		
$KMnO_4$, V_1	6.325	mL	0.024	mol/L
$K_2C_2O_4$, m_2	0.0513	g		
$KMnO_4$, V_1	6.45	mL	0.024	mol/L
$K_2C_2O_4$, m_3	0.0522	g		
$KMnO_4$, V_1	6.6	mL	0.024	mol/L
AVERAGE CONCENTRATION			**0.024**	**mol/L**

Appendix E Inhibitor and buffer calculations

Sampling for TOC

The syringes for the TOC samples contained 2mL of inhibitor and were filled with 6mL of sample. To verify that the hydrogen peroxide was completely removed the following calculations were made. Molar masses are were found in SI chemical data[51].

H_2O_2-removal: The amounts of the two oxidant scavengers were calculated:

$$n_{I^-} = C_{I-} \cdot V_{inhibitor} = 0.10\frac{mol}{L} \cdot 0.002L = \underline{0.0002\frac{mol}{sample}}$$

$$n_{Na_2SO_3} = C_{Na_2SO_3} \cdot V_{inhibitor} = 0.10\frac{mol}{L} \cdot 0.002L = \underline{0.0002\frac{mol}{sample}}$$

Thereafter the amounts of hydrogen peroxide for the two concentrations used were calculated:

$$n_{2xH_2O_2} = \frac{V_{2xH_2O_2} \cdot x_{H_2O_2} \cdot \rho_{30\%H_2O_2}}{M_{H_2O_2} \cdot V_{Sample}} = \frac{2.86mL_{30\%H_2O_2} \cdot 0.3\frac{g_{H_2O_2}}{g_{30\%H_2O_2}} \cdot 1.1\frac{g_{30\%H_2O_2}}{mL_{30\%H_2O_2}}}{34.015\frac{g_{H_2O_2}}{mol_{H_2O_2}} \cdot 6mL_{sample}} = \underline{0.00017\frac{mol}{sample}}$$

$$n_{10xH_2O_2} = 5 \cdot n_{2xH_2O_2} = \underline{0.00083\frac{mol}{sample}}$$

Iron precipitation: The final iron content of the mixed inhibitor and the sample found. Firstly the initial concentration of phosphate ions was calculated:

$$C_{PO_4^{3-}} = \frac{C^0_{PO_4^{3-}} \cdot V_{Inhibitor}}{V_{Inhibitor} + V_{sample}} = \frac{[0.05 + 0.05]\frac{mol}{L} \cdot 2mL}{2mL + 6mL} = \underline{0.025\frac{mol}{L}}$$

Thereafter the assumption was made that the iron content in the reactor was a lot smaller, so that the phosphate concentration would not change much. The final iron concentration was found by using the solubility constant cited[42]:

$$C_{m,Fe3+} = \frac{M_{Fe3+}}{C_{PO_4^{3-}} \cdot Ksp} = \frac{58485\frac{mg}{mol}}{0.025\frac{mol}{L} \cdot 5 \cdot 10^{10}\frac{L^2}{mol^2}} = \underline{4.7 \cdot 10^{-5}\frac{mg}{L}}$$

Sampling for HPLC

The same calculation was done for the HPLC samples with the buffer, obtaining a final iron concentration of:

$$C_{m,Fe3+} = \left[C_{PO_4^{3-}} \right]^{-1} \cdot \frac{M_{Fe3+}}{Ksp} = \left[\frac{[0,05+0,05]\frac{mol}{L} \cdot 0,6mL}{0,6mL+1,4mL} \right]^{-1} \frac{58485\frac{mg}{mol}}{5 \cdot 10^{10}\frac{L^2}{mol^2}} = \underline{3.90 \cdot 10^{-5}\frac{mg}{L}}$$

Calculations done after leached iron measurements:

The maximum iron content was found to be 4mgL^{-1}. The inhibitor and buffer solution remove therefore approximately 100 % of the iron.

Converting the mass concentration into molar concentration gives:

$$C_{Fe^{3+}} = \frac{4\frac{mg}{L}}{58485\frac{mg}{mol}} = \underline{6.84 \cdot 10^{-5}\frac{mol}{L}}$$

This confirms the earlier assumption that the iron content was negligible compared to the phosphate concentration.

Appendix F HPLC curves

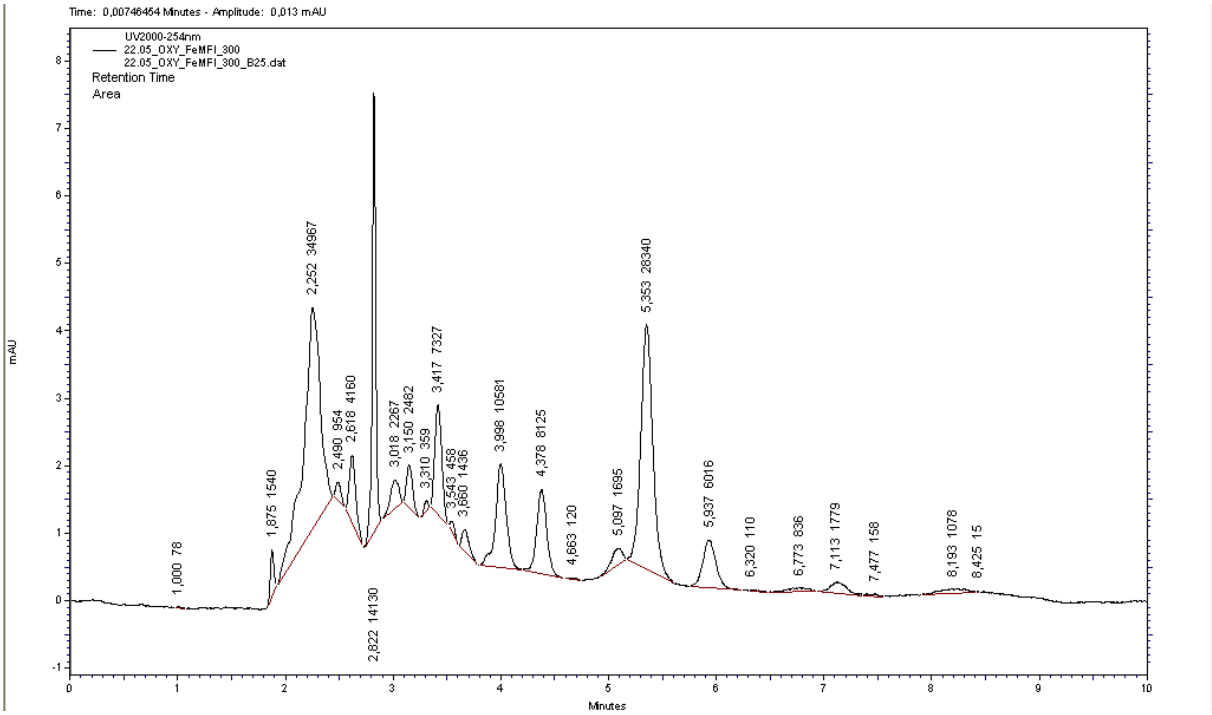

Figure F-1: HPLC curve after 300 minutes of oxidation. Fe/MFI - 45°C – 2x H_2O_2

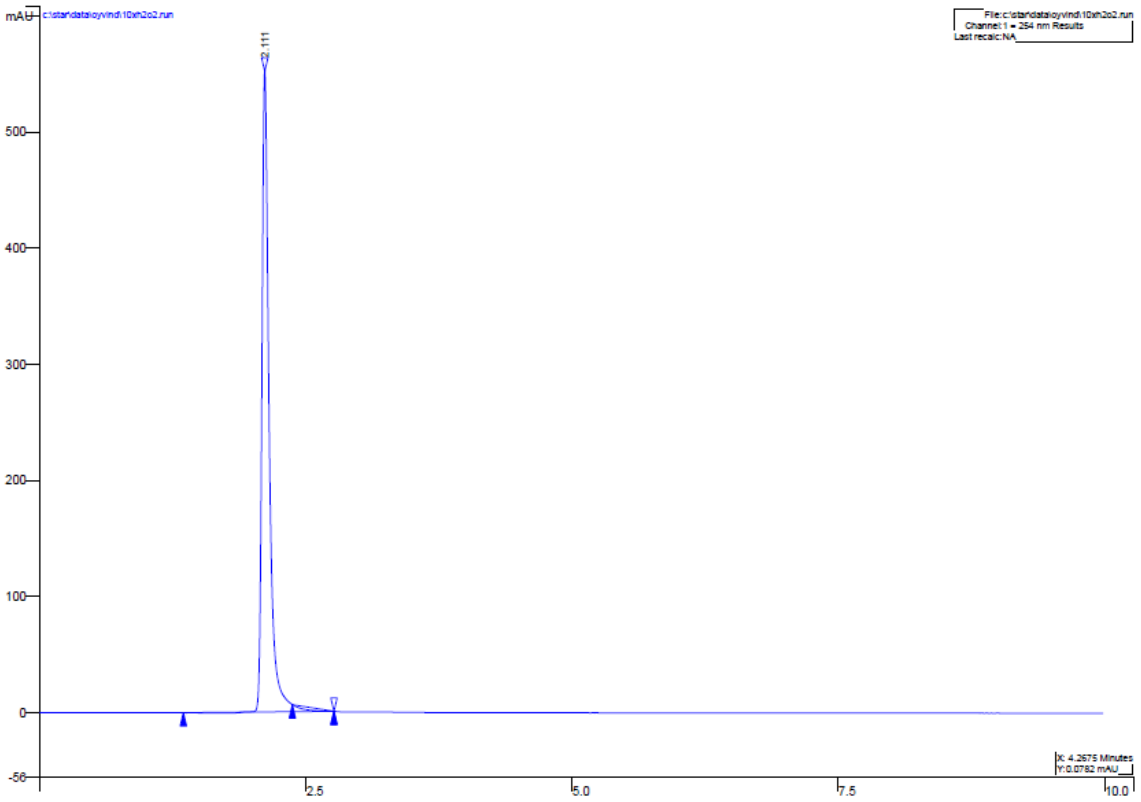

Figure F-2: 10 times the stoechiometry of H_2O_2 run with the fast analysis for paracetamol

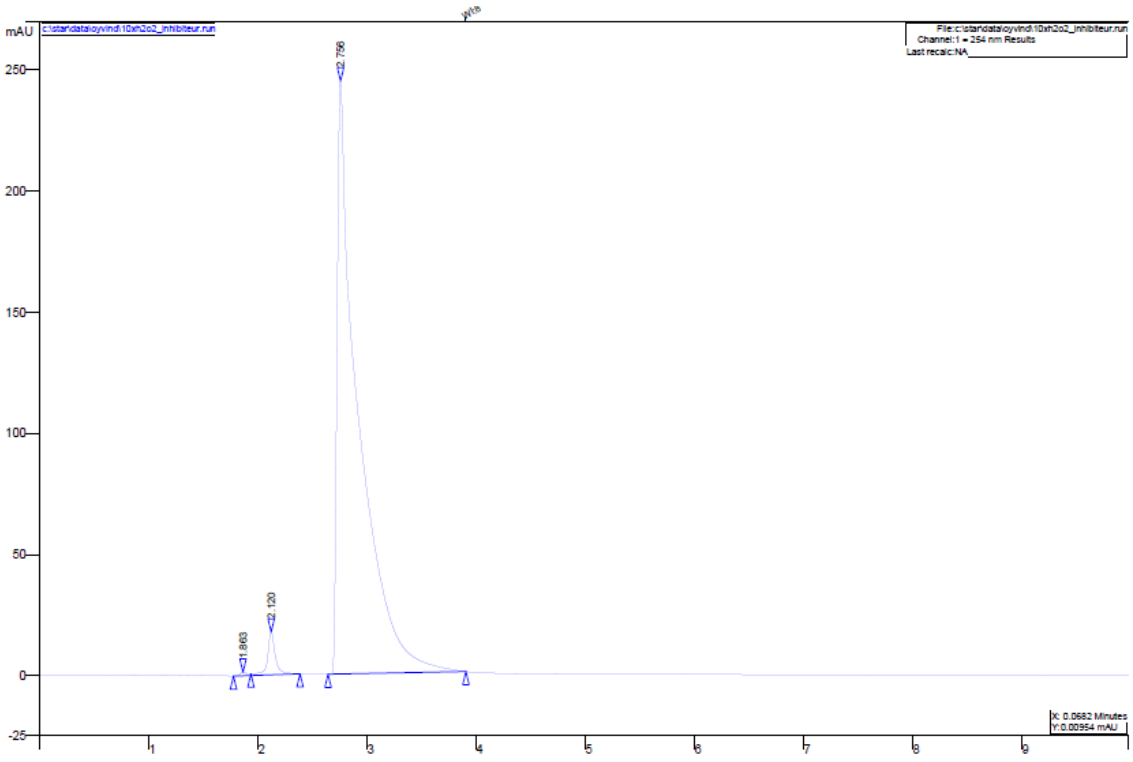

Figure F-3: Ten times the stoechiometry of H_2O_2 with inhibitor run with the fast analysis for paracetamol, clearly showing that the peak of H_2O_2 is removed by the inhibitor solution

Appendix G Assumptions

Assumption 1: All sample dilutions were based on weight, while all the initial concentrations and results were based on volume. This was done to reduce the time of sample preparations and avoid the smallest fluctuations in density with regards to atmospheric pressure. Hence it was assumed that: one milliliter equaled one gram for all the solutions regarding the sample preparations. This assumption is controlled theoretically under, including the theoretical density of each solution in the calculations.

The concentration of paracetamol was obtained from the HPLC by using the following equation:

$$C_{Paracetamol} = K_{Dillution,HPLC} \cdot \frac{A_{Area,HPLC}}{K'_{calibrationcurve,HPLC}}$$

The concentration of TOC was obtained by using the following equation:

$$C_{TOC} = K_{Dillution,TOC} \cdot A_{Area,TOC} \cdot K_{calibrationcurve,TOC}$$

The mass/volume based assumption affects the dilution factor K. The theoretical error estimated by finding the volume based dilution factor:

$$K^{V}_{dillution,HPLC} = \frac{\frac{m_{sample}}{\rho_{sample}} + \frac{m_{buffer}}{\rho_{buffer}}}{\frac{m_{sample}}{\rho_{sample}}} = 1 + \frac{m_{buffer}}{m_{sample}} \cdot \frac{\rho_{sample}}{\rho_{buffer}}$$

And dividing this volume based dilution factor by the mass based dilution factor used in calculations:

$$\frac{K^{V}_{dillution,HPLC}}{K^{m}_{dillution,HPLC}} = \frac{1 + \frac{m_{buffer}}{m_{sample}} \cdot \frac{\rho_{sample}}{\rho_{buffer}}}{1 + \frac{m_{buffer}}{m_{sample}}}$$

Regarding the TOC values, the volume based dilution factor can be found in this manner:

$$K^{V}_{dillution,TOC} = \frac{\frac{m_{sample}}{\rho_{sample}} + \frac{m_{inhibitor}}{\rho_{inhibitor}}}{\frac{m_{sample}}{\rho_{sample}}} \cdot \frac{\frac{m_{dillution}}{\rho_{dillution}}}{\frac{m_{filtrat}}{\rho_{filtrat}}} = \left(1 + \frac{m_{inhibitor}}{m_{sample}} \cdot \frac{\rho_{sample}}{\rho_{inhibitor}}\right) \cdot \frac{m_{dillution}}{m_{filtrat}} \cdot \frac{\rho_{filtrat}}{\rho_{dillution}}$$

Afterwards dividing it by the mass based dilution factor:

$$\frac{K^{V}_{dillution,TOC}}{K^{m}_{dillution,TOC}} = \frac{\left(1+\frac{m_{inhibitor}}{m_{sample}}\cdot\frac{\rho_{sample}}{\rho_{inhibitor}}\right)\cdot\frac{m_{dillution}}{m_{filtrat}}\cdot\frac{\rho_{filtrat}}{\rho_{dillution}}}{\left(1+\frac{m_{inhibitor}}{m_{sample}}\right)\cdot\frac{m_{dillution}}{m_{filtrat}}}$$

The values presented in Table G-1 were calculated assuming that the added salts did not have any volume and that water has a density of 1000 gL^{-1}. The values for the different masses were found by doing an average over 15 values measured in the experiments.

Table G-1: Density and mass values used to evaluate the mass based dilution factor

	Symbol	Quantity	
Density sample. dillution	ρ_{sample}. $\rho_{dillution}$	1000	g/L
Density inhibitor solution	$\rho_{inhibitor}$	1050	g/L
Density buffer solution	ρ_{buffer}	1021	g/L
Density filtrat	$\rho_{filtrat}$	1013	g/L
Sample mass HPLC	m_{sample}	1.68	g
Buffer mass	m_{buffer}	0.58	g
Sample mass TOC	m_{sample}	5.44	g
Inhibitor mass	$m_{inhibitor}$	1.99	g
Filtrat mass	$m_{filtrat}$	6.37	g
Dillution	$m_{dillution}$	25.07	g

The results of these calculations were:

$$\frac{K^{V}_{dillution,HPLC}}{K^{m}_{dillution,HPLC}} = \underline{0.995}$$

And

$$\frac{K^{V}_{dillution,TOC}}{K^{m}_{dillution,TOC}} = \underline{1.000}$$

These differences in dilution factors were so small, that using a mass based system would have little effect on the outcome of the results.

Assumption 2: It was also assumed that the volume of samples taken was not interfering with the reaction. All the samples that were extracted before the addition of the oxidant would result in a higher oxidant concentration than expected. The total volume of samples taken before this was:

$$V_{samples} = 2x8mL + 3x2mL = \underline{22mL}$$

This resulted in an actual oxidant concentration superior to the theoretical. The difference was: 4.4%, 2.2% and 1.5% for the 0.5, 1 and 1.5L reactor setup respectively. As this method was used for all experiments and there was little difference between the reactors the assumption was validated.

Appendix H Adsorption equilibrium for the photo-Fenton

The calculation of the delay of zeolite concentration equilibrium between the reactors was simulated in Excel, by using the discretized equation for the conservation of mass[52] under.

$$C_{1,i+1} \cdot V_1 = C_{1,i} \cdot V_1 + \frac{\Delta V}{\Delta x}\left(C_{2,i-10} - C_{1,i}\right)$$

$$C_{2,i+1} \cdot V_2 = C_{2,i} \cdot V_2 + \frac{\Delta V}{\Delta x}\left(C_{1,i-10} - C_{2,i}\right)$$

The "*i-10*" index represents the delay of the pump debit, due to the length of the tube. Listed in Table H-1were the parameter values that were used.

Table H-1: Parameters used for the simulation of the equilibrium between the photo-Fenton reactors

Parameter name	Parameter symbol	Value	Denomination
Volume of reactor 1	V_1	1	L
Volume of reactor 2	V_2	0.5	L
Initial concentration of reactor 1	$C_{1,0}$	3	gL^{-1}
Initial concentration of reactor 2	$C_{2,0}$	0	gL^{-1}
Flow of the pump	$\frac{\Delta V}{\Delta x}$	0.00121	$Lsec^{-1}$
Step size	i	1	sec
Interval	$[i_{min}, i_{max}]$	0-1600	sec

The result of the simulation was plotted, and the equilibrium was found around 1200 seconds (20 minutes), see Figure H-1.

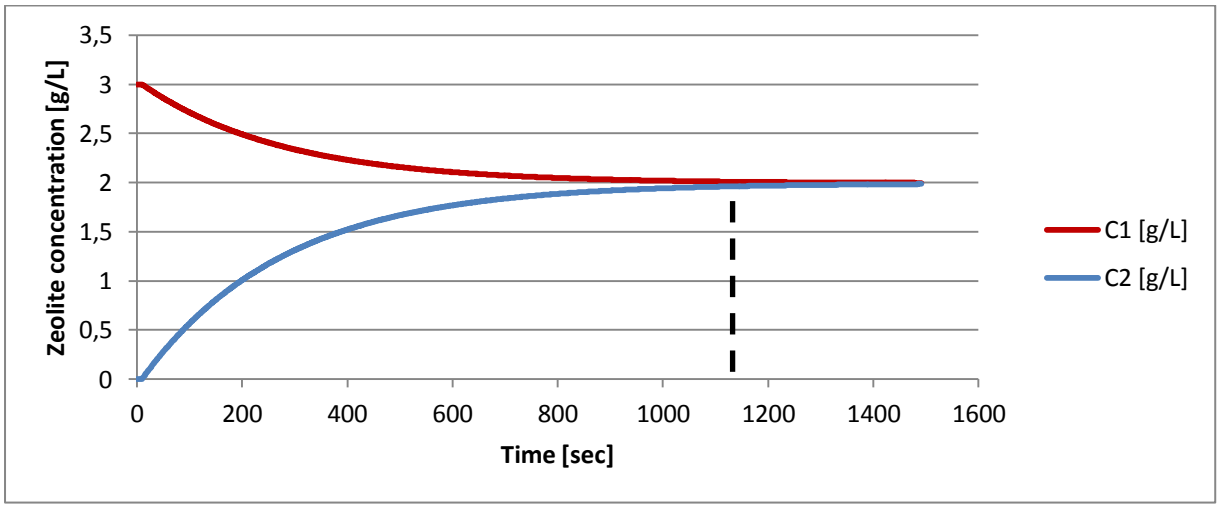

Figure H-1: Simulation of the delay of the zeolite concentration equilibrium between the reactors

Appendix I Statistical uncertainty for the TOC values

The TOC values plotted in section 4.3 are presented with the sum of statistical errors. These are calculated in each case with the statistical errors from the sample preparation and the TOC apparatus. The TOC values are calculated in the following manner:

$$C_{TOC}^{true} = \left(C_{TC} - C_{IC}\right) \cdot \left(\frac{m_{solution+inhibitor}}{m_{solution}} \cdot \frac{m_{dillution}}{m_{filtrate}} \right)$$

To calculate the statistical error the Gaussian error propagation formula is used

$$\sigma_{\varphi} = \sqrt{\sum_{i=1}^{n} \left(\frac{\partial \varphi}{\partial \chi_i} \right)^2 \sigma_{\chi_i}^2}$$

Where σ_{φ} is the sum of statistical errors of the main function φ. χ_i are the parameters of the main function with each their statistical errors, σ_{χ}. With some definitions:

$$C_{TOC} = \left(C_{TC} - C_{IC}\right), C_D = \left(\frac{m_{solution+inhibitor}}{m_{solution}} \cdot \frac{m_{dillution}}{m_{filtrate}} \right)$$

The sum of the statistical errors for the TOC values are calculated by the following formula:

$$\sigma_{C_{TOC}^{true}} = \sqrt{\left(\frac{\partial C_{TOC}^{true}}{\partial C_{TC}} \right)^2 \sigma_{C_{TC}}^2 + \left(\frac{\partial C_{TOC}^{true}}{\partial C_{IC}} \right)^2 \sigma_{C_{IC}}^2 + \left(\frac{\partial C_{TOC}^{true}}{\partial m_{sol+inh}} \right)^2 \sigma_{m_{sol+inh}}^2 + \left(\frac{\partial C_{TOC}^{true}}{\partial m_{sol}} \right)^2 \sigma_{m_{sol}}^2 + \left(\frac{\partial C_{TOC}^{true}}{\partial m_{filtrate}} \right)^2 \sigma_{m_{filtrate}}^2 + \left(\frac{\partial C_{TOC}^{true}}{\partial m_{dillution}} \right)^2 \sigma_{m_{dillution}}^2}$$

$$\frac{\partial C_{TOC}^{true}}{\partial C_{TC}} = C_A, \sigma_{C_{TC}} = 0.02 \cdot C_{TC}$$

$$\frac{\partial C_{TOC}^{true}}{\partial C_{IC}} = -C_A, \sigma_{C_{IC}} = 0.02 \cdot C_{IC}$$

$$\frac{\partial C_{TOC}^{true}}{\partial m_{sol+inh}} = C_{TOC} \cdot C_A \cdot \frac{1}{m_{sol+inh}}, \sigma_{m_{sol+inh}} = 0,0001$$

$$\frac{\partial C_{TOC}^{true}}{\partial m_{sol}} = -C_{TOC} \cdot C_A \cdot \frac{1}{m_{sol}}, \sigma_{m_{sol}} = 0,0001$$

$$\frac{\partial C_{TOC}^{true}}{\partial m_{filtrate}} = -C_{TOC} \cdot C_A \cdot \frac{1}{m_{filtrate}}, \sigma_{m_{filtrate}} = 0,0001$$

$$\frac{\partial C_{TOC}^{true}}{\partial m_{dillution}} = C_{TOC} \cdot C_A \cdot \frac{1}{m_{dillution}}, \sigma_{m_{dillution}} = 0,0001$$